




A FISH AND TETRAPOD FAUNA FROM ROMER'S GAP PRESERVED IN SCOTTISH TOURNAISIAN FLOODPLAIN DEPOSITS

by BENJAMIN K. A. OTOO^{1,5,*} , JENNIFER A. CLACK^{1,*}, TIMOTHY R. SMITHSON¹, CARYS E. BENNETT², TIMOTHY I. KEARSEY³ and MICHAEL I. COATES⁴

¹University Museum of Zoology Cambridge, Downing Street, Cambridge, CB2 3EJ, UK; jac18@cam.ac.uk, ts556@cam.ac.uk

²Department of Geology, University of Leicester, Leicester, LE1 7RH, UK; ceb28@leicester.ac.uk

³British Geological Survey, The Lyell Centre, Research Avenue South, Edinburgh, EH14 4AP, UK; timk1@bgs.ac.uk

⁴Committee on Evolutionary Biology, University of Chicago, Culver Hall, 1025 East 57th Street, Chicago, IL 60637, USA; mcoates@uchicago.edu

⁵Current address: Committee on Evolutionary Biology, University of Chicago, Culver Hall, 1025 East 57th Street, Chicago, IL 60637, USA; botoo@uchicago.edu

*Corresponding authors

Typescript received 15 December 2017; accepted in revised form 20 July 2018

Abstract: The end-Devonian mass extinction has been framed as a turning point in vertebrate evolution, enabling the radiation of tetrapods, chondrichthyans and actinopterygians. Until very recently 'Romer's Gap' rendered the Early Carboniferous a black box standing between the Devonian and the later Carboniferous, but now new Tournaisian localities are filling this interval. Recent work has recovered unexpected tetrapod and lungfish diversity. However, the composition of Tournaisian faunas remains poorly understood. Here we report on a Tournaisian vertebrate fauna from a well-characterized, narrow stratigraphic interval from the Ballagan Formation exposed at Burnmouth, Scotland. Microfossils suggest brackish conditions and the sedimentology indicates a low-energy debris flow on a vegetated floodplain. A range of vertebrate bone sizes are preserved. Rhizodonts are represented by the most material, which can be assigned to two taxa. Lungfish are represented by several species, almost all

of which are currently endemic to the Ballagan Formation. There are two named tetrapods, *Aytonerpeton* and *Diplo-radus*, with at least two others also represented. Gyracanthids, holocephalans, and actinopterygian fishes are represented by rarer fossils. This material compares well with vertebrate fossils from other Ballagan deposits. Faunal similarity analysis using an updated dataset of Devonian–Carboniferous (Givetian–Serpukhovian) sites corroborates a persistent Devonian/Carboniferous split. Separation of the data into marine and non-marine partitions indicates more Devonian–Carboniferous faunal continuity in non-marine settings compared to marine settings. These results agree with the latest fossil discoveries and suggest that the Devonian–Carboniferous transition proceeded differently in different environments and among different taxonomic groups.

Key words: Romer's Gap, Tournaisian, tetrapod, floodplain, Carboniferous, rhizodont.

ROMER'S Gap (Romer 1956; Coates & Clack 1995) is a hiatus in the non-marine fossil record that currently spans the Tournaisian stage of the Carboniferous (~359–345 Ma). Named for the paucity of tetrapod fossils throughout this interval, the gap has long obscured cladogenic events and ecological transitions implied by differences between the few, mostly aquatic, limbed forms present at the end of the Devonian and the diverse and disparate tetrapods known from the Visean (Wellstead 1982; Clarkson *et al.* 1994; Pardo *et al.* 2017). What little we know of Tournaisian tetrapods is drawn from not much more than isolated bones and fragments from localities such as Blue Beach in Canada (Anderson *et al.*

2015), but with the notable exception of the unique, substantial and partly articulated skeleton of *Pederpes* from Scotland (Clack & Finney 2005). However, the challenge presented by Romer's Gap extends beyond tetrapods. Few Tournaisian fish localities have been known until recently (Clarkson 1985; Long 1989; Sallan & Coates 2010; Mansky & Lucas 2013; Sallan & Galimberti 2015; Mickle 2017; Richards *et al.* 2018), and these, too, appear impoverished relative to subsequent Visean faunas.

It follows that all three major living vertebrate divisions, actinopterygians (Sallan 2014; Giles *et al.* 2017), chondrichthyans (Coates *et al.* 2017, 2018), and tetrapods (Clack *et al.* 2016; Pardo *et al.* 2017) underwent major

radiations within this key interval. Moreover, it seems likely that these radiations occurred opportunistically, to refill ecological space in the aftermath of serial extinction events that occurred close to end of the Devonian (Sallan & Coates 2010; Sallan & Galimberti 2015). But the absence of a substantial record of Tournaisian fossil vertebrates obscures the timing and true phylogenetic pattern of the Devonian–Carboniferous transition. It remains unclear whether these large-scale post-extinction diversifications arose from short (Tournaisian) or long (Devonian) fuses. We have almost no perspective on the multiple ecological transitions that took place at this time, especially the ongoing vertebrate invasions of non-marine environments including the likely multiple episodes of terrestrialization within the Tetrapoda. Moreover, the hypothesized abruptness of the end-Devonian mass extinction (Hangenberg event) (Sallan & Coates 2010) and an inferred Lilliput effect (Sallan & Galimberti 2015) deserve to be tested. Already, Tournaisian tetrapod discoveries include a mix of morphologies (Anderson *et al.* 2015) that are distributed across multiple nodes in recent phylogenetic analyses (Clack *et al.* 2016) and a recently-recognized Tournaisian radiation in lungfish (Smithson *et al.* 2015) contradicts a historical narrative of post-Devonian decline and stasis.

These various observations raise the possibility that the Devonian–Carboniferous divide recovered by Sallan & Coates (2010) might not be expressed in the same way across all environments, particularly given the uneven distribution of end-Devonian diversity loss among taxonomic groups (Sallan & Coates 2010). Thus, there may be discernable time/environment associations, with different levels of taxonomic/ecological continuity across the Devonian–Carboniferous boundary. However, widespread euryhalinity among Devonian–Carboniferous vertebrates (Ó Gogáin *et al.* 2016; Goedert *et al.* 2018) may support the hypothesis of a cosmopolitan post-extinction fauna in the Tournaisian (Friedman & Sallan 2012).

Here we describe the vertebrate fossil fauna from the Tournaisian-age Ballagan Formation exposed on the beach at Burnmouth, Scotland. The fossils come from a 1 m stratigraphic interval. These new data, along with those from the Blue Beach locality (Anderson *et al.* 2015), are added to the dataset of Sallan & Coates (2010) to test their conclusions of a Devonian/Carboniferous faunal divide against new Tournaisian data.

GEOLOGICAL CONTEXT

The Ballagan Formation crops out in northern England and the Midland Valley of Scotland. It has previously been referred to as the Cementstone Group in England and the lower part of the Calciferous Sandstone Measures

in Scotland (Greig 1988), and probably spans the whole of the Tournaisian (Smithson *et al.* 2012). The Ballagan is characterized by alternating dolostones ('cementstones'), palaeosols, sandstones and siltstones. The last of these have been identified as an important facies for preserving fossils both in the Ballagan and elsewhere in the Carboniferous (Bennett *et al.* 2016; Kearsley *et al.* 2016). The Ballagan has produced isolated (macro)fossils in the past (Clack 2002) but its full fossiliferous potential has only been realized recently via the TW:eed project (<http://tetrapods.org/>), which has also increased our sedimentological and palaeoenvironmental knowledge of the formation (Smithson *et al.* 2012, 2015; Bennett *et al.* 2016, 2017; Clack *et al.* 2016; Kearsley *et al.* 2016).

The entire Ballagan Formation is exposed at Burnmouth, Scotland (Fig. 1), as just over 500 m of vertically dipping beds. Most of the tetrapod fossils at Burnmouth occur from 332–383 m, though there are isolated bones known from lower horizons (see Clack *et al.* 2016, fig. 6a). The greatest concentration comes from a ~50 cm span within a highly-sampled 1 m interval at 340.5 m originally discovered by TRS. This 1 m interval contains the *Ossirarus* and *Aytonerpeton* beds (Clack *et al.* 2016) and is here designated the Tetrapod Interval Metre, or TIM (Fig. 2).

The Ballagan Formation comprises 10 facies and three facies associations, each of which occur throughout the formation: (1) fluvial facies association; (2) overbank facies association; and (3) saline-hypersaline lake facies association (Bennett *et al.* 2016). The sandy siltstone facies occurs within the overbank facies association, and is characterized as matrix-supported, ungraded siltstones, with millimetre-sized siltstone and very fine sandstone lithic clasts. This facies is a key characteristic of the Ballagan Formation, with 71 beds reported from the Burnmouth succession. Beds are randomly distributed through the succession, laterally variable, and range in thickness from 0.2 to 140 cm (Bennett *et al.* 2016). 71% of beds overlie palaeosols or desiccation cracks and often occur in stacked sequences with palaeosols. The palaeosols are rooted red, green or grey siltstones and only rarely contain small carbonate nodules (Kearsley *et al.* 2016). They represent a range of floodplain environments including woodland (vertisols), scrubby vegetation (entisols, inceptisols) and saline marshes (gleyed inceptisols).

The sandy siltstone beds are interpreted as having formed as a cohesive flow resulting from monsoonal-type flood events, picking up sediment clasts and fossil material from desiccated floodplain lakes and vegetated ground as the flood travelled (Bennett *et al.* 2016). The beds either deposited material in depressions on a dry vegetated floodplain, or into existing floodplain lakes or pools. The high degree of vertebrate and invertebrate fossil articulation within these units indicates a local origin

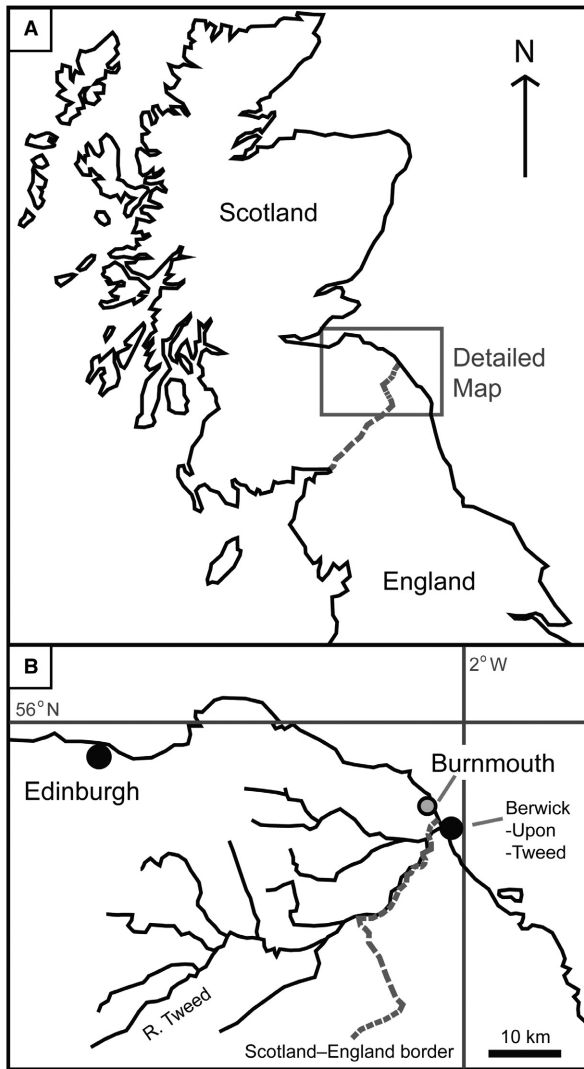


FIG. 1. A, map showing English/Scottish border. B, the detailed location of the study area at Burnmouth. Modified from Kearsy *et al.* (2016).

and minimal transport of the fossil components (Bennett *et al.* 2016).

MATERIAL AND METHOD

Collection and preparation

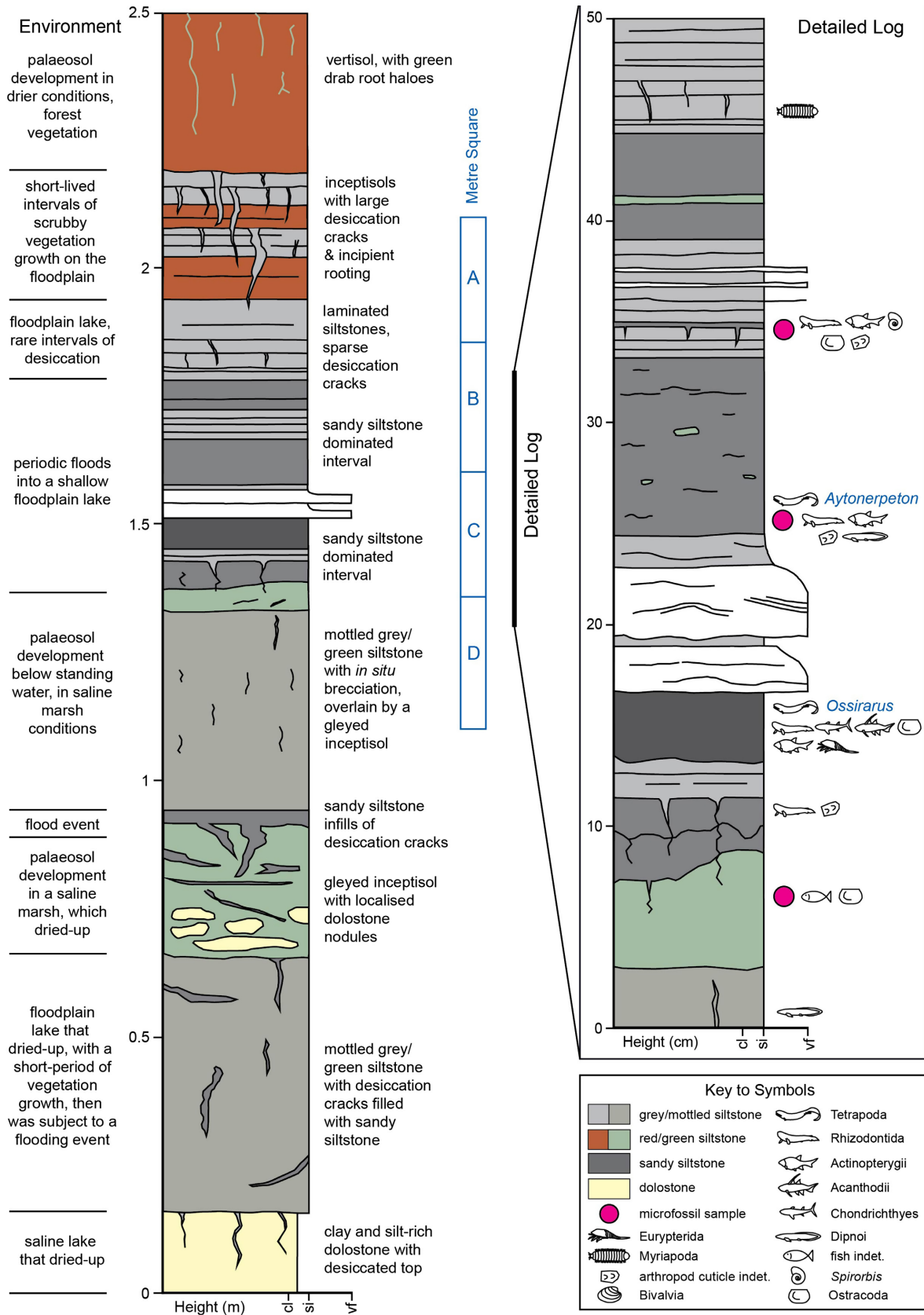
A detailed sedimentary log of the section in the cliff exposure was drawn in October 2012 and enhanced by additional observations gathered from summer fieldwork in 2013–2016. Samples were taken approximately every 20 cm through the studied interval and their fossil content was examined under a Leica binocular microscope at the University of Leicester. Initial fossil observations from

all sandy siltstone beds identified at Burnmouth (including those in this interval) are recorded in Bennett *et al.* (2016, appendix 1). To obtain a high-resolution sedimentological and palaeontological data set, the TIM was sampled by removing a 1 m × 1 m × 30 cm block from the foreshore. This was recovered in June 2013, with permission from Crown Estate Scotland and Scotland Natural Heritage. This sample, was divided into four equal units 25 × 25 × 30 cm long-wide-deep, named A–D from left to right and 1–3 from top to bottom. From here the fossil content was recorded. Macrofossil material presented here includes samples collected from the TIM by S. P. Wood in 2007, TRS in 2006–2008, and by the TW:eed team in 2012–2013, and material prepared from the metre-square block in 2014–2015 by SPW, TRS, JAC and BKAO. Much of this collecting was done approximately 18 m laterally seaward from the metre square.

The fossils of the TIM were initially revealed using a 200 g hammer and cold chisel. These were then prepared using a mounted tungsten-carbide needle, under binocular microscopes with up to ×50 objectives. Dilute Paraloid B72 was used as a specimen consolidant during preparation. Specimen photography was carried out using a Panasonic Lumix DMC-LZ5 and a Sony Cyber-shot DSC-RX100 III digital camera and a Dino-Lite Pro/Pro2 AD4000 AM4000 digital microscope. Image processing was carried out in Adobe Photoshop CS6. Select specimens were CT scanned using a Nikon Metrology XT H 225 ST High Resolution CT Scanner at the University of Cambridge Biotomography Centre. The following parameters were used: isotropic voxel size 0.0609 mm, 1080 projections, no filter, X-ray 120 kV, 125 μA, 1789 slices, 1000 ms per slice exposure, 24 dB gain. 3-D sectioning was carried out in Mimics Innovation Suite (Materialise, Leuven, Belgium; <https://www.materialise.com/en/medical/software/mimics>). Additional rendering and manipulation of objects was done in Meshlab (Visual Computing Lab-ISTI-CNR; <http://www.meshlab.net/>).

Micropalaeontological analysis

Three beds from the TIM were selected for micropalaeontological processing from three different facies (Fig. 3): (1) palaeosol facies, a gleyed inceptisol that occurs just below the main fossil-bearing unit; (2) sandy siltstone facies, within the tetrapod-bearing unit; (3) laminated grey siltstone facies, with desiccation cracks containing sandy siltstone, above the tetrapod-bearing unit. All three facies are part of the overbank facies association (Bennett *et al.* 2016). Approximately 15–20 g of each sample was processed overnight in a 5% solution of hydrogen peroxide, then wet sieved at 1000, 425, 250, 125, 65 μm fractions and oven dried at 40°C. All fossil specimens present



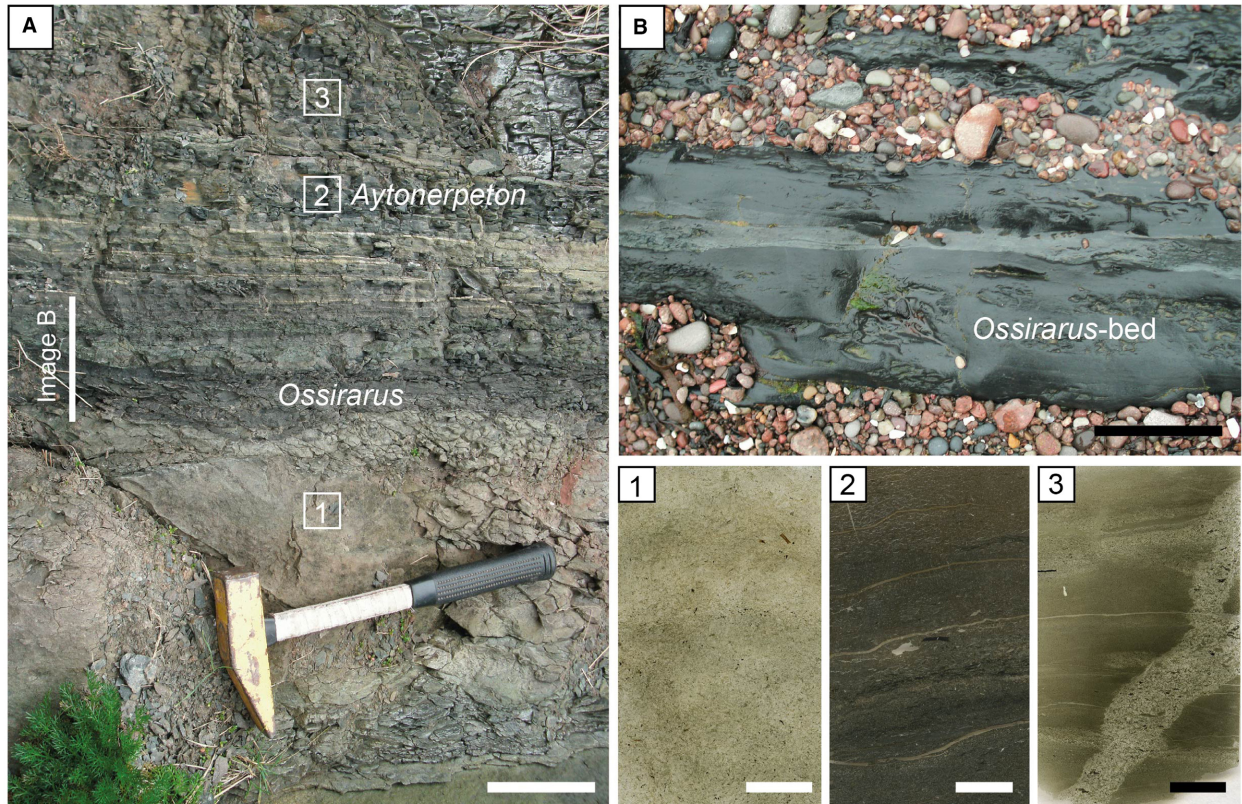


FIG. 3. Tetrapod-bearing bed exposure at Burnmouth. A, photograph of the cliff section, with position of the *Ossirarus*, *Aytoneperpeton* and microfossil sample beds (1–3). B, the *Ossirarus*-bed exposed on the foreshore at Burnmouth. 1–3, thin section scans of beds that were processed for microfossils: 1, palaeosol; 2, sandy siltstone; 3, laminated grey siltstone. Scale bars represent: 10 cm (A); 5 cm (B); 5 mm (1–3). Colour online.

were picked from the 1000, 425, 250 and 125 μm fractions and total counts recorded (Otoo *et al.* 2018, micropalaeontology data). Three standard-sized, polished thin sections (20 μm thick) of these beds were examined on a Leica petrographic microscope at the University of Leicester.

Faunal analyses

Sallan & Coates (2010) compiled a large dataset of gnathostome vertebrate fossil occurrences from the Middle Devonian (Givetian stage) through to the end of the Early Carboniferous (Serpukhovian stage). This dataset was updated to include new data from the Burnmouth TIM fauna (named 'Burnmouth-TIM' in the analyses), Blue Beach (Brazeau 2005; Mansky & Lucas 2013;

Anderson *et al.* 2015) and Mill Hole (Carpenter *et al.* 2014), as well as revisions of rhizodont taxonomy (Johansson & Ahlberg 2001; Jeffery 2006). Localities were characterized as marine, marginal or non-marine, with more specific environmental categories based on descriptions in the original dataset and literature. Both raw diversity (number of species in each taxonomic group) and relative diversity (taxon diversity relative to locality diversity) were analysed. This accounted for the effects of assemblage size and provided comparability with the Sallan & Coates (2010) analyses.

All faunal analyses were run in PAST (Hammer 2015). In each analysis, sites were not grouped *a priori* by stage or environment. Correspondence analysis (CA) was used to recover any time–environment faunal associations and investigate which taxa were driving similarities and differences between faunas. Diversity datasets

FIG. 2. Sedimentary log of the tetrapod-bearing beds at Burnmouth. The 250 cm-height log represents the exposure on the foreshore, while the detailed log covers part of the sampled metre square. Fossil symbols illustrated on the metre square relate to those identified in hand specimen and from microfossil samples.

are presented in Otoo *et al.* (2018). Non-parametric multidimensional scaling (NMDS) was used to characterize faunal similarity quantitatively and graphically using Bray–Curtis distance, a faunal similarity metric (Bray & Curtis 1957).

Institutional abbreviations. UMZC, University of Cambridge Museum of Zoology, UK; NMS, National Museums Scotland, Edinburgh, Scotland, UK; GLAHM, Hunterian Museum, Glasgow, Scotland, UK; YMP, Yale Peabody Museum of Natural History, New Haven, Connecticut, USA; NSM, Nova Scotia Museum of Natural History, Halifax, Nova Scotia, Canada; NBMG, New Brunswick Museum (Geology), Saint John, New Brunswick, Canada.

SYSTEMATIC PALAEOLOGY

Macrofossil distribution

The greatest portion of macrofossils from the TIM come from section C (Fig. 2). The microfossil assemblage of Sample 3 (see Microfossil results) occurs within the same lithology as the TIM and has similar microfossil content to the TIM macrofossil content. However, macrofossils have been found elsewhere within the TIM, including the palaeosol/*Ossirarus* bed (a lungfish body fossil) and the laminated grey siltstone (eurypterid fossils; Smithson *et al.* 2012).

Faunal list

A full list of vertebrate taxa represented within the TIM is presented in Table 1. The following taxa and material have been described elsewhere and will not be included here: *Aytonerepeton microps* (Clack *et al.* 2016), *Diploradus austiumensis* (Clack *et al.* 2016), *Ballagadus rossi* (Smithson *et al.* 2015). The indeterminate tetrapod material is figured in the supplement to Clack *et al.* (2016) and, based on tooth morphology, probably represents at least two different taxa but is not described here.

Class CHONDRICHTHYES Huxley, 1880
Family GYRACANTHIDAE *sensu* Warren *et al.*, 2000
GYRACANTHIDAE *indet.*

Material. Numerous fin spines, as well as UMZC 2017.2.584 and UMZC 2017.2.582, two scapulocoracoids (Fig. 4).

Diagnosis. Large, broad-based paired fin spines having a distinct longitudinal curvature; fin spines inserted deep into the body, their exerted portions with ornament

TABLE 1. Summary list of vertebrate taxa from the TIM at Burnmouth.

Class ACANTHODII
Family GYRACANTHIDAE
Gyracanthidae <i>indet.</i>
Class CHONDRICHTHYES
Chondrichthyes <i>indet.</i>
Superorder HOLOCEPHALI
Order MENASPIFORMES
aff. Menaspiformes
Class OSTEICHTHYES
Subclass SARCOPTERYGII
Order RHIZODONTIDA
cf. <i>Strepsodus sauroides</i>
aff. <i>Archichthys portlocki</i>
Order DIPNOI
Dipnoi <i>indet.</i>
<i>Uronemus splendens</i>
<i>Ctenodus roberti</i>
<i>Xylognathus macrustenus</i>
<i>Ballagadus rossi</i> (Smithson <i>et al.</i> 2015)
Superclass TETRAPODA
<i>Aytonerepeton microps</i> (Otoo, Clack & Smithson <i>in</i> Clack <i>et al.</i> , 2016)
<i>Diploradus austiumensis</i> (Clack & Smithson <i>in</i> Clack <i>et al.</i> , 2016)
aff. <i>Pederpes</i> and <i>Whatcheeria</i>
Tetrapoda <i>indet.</i> (at least two taxa, Clack <i>et al.</i> 2016)
Class ACTINOPTERYGII Cope 1887
Actinopterygii <i>indet.</i>

Taxa with material that has been described elsewhere are listed with the appropriate reference.

ridges oblique to the long axis of the spine. Fin spine ridges bearing tubercular ornament. Large triangular scapulocoracoid forms part of pectoral girdle.

Description. The spines thus far collected from the TIM have the distinctive curvature of gyracanthid pectoral spines, as opposed to the straightness of spines from other parts of the body (Warren *et al.* 2000). Consistent with Warren *et al.*'s diagnosis (see above) at least 20 oblique ridges intersect the boundary of the insertion area. Unlike *Gyracanthides murrayi* (Warren *et al.* 2000), the insertion area is smooth to gently striated. Tubercles on the oblique ridges are triangular with a median ridge. Oblique ridges closest to the leading edge of spine insertion have 2 tubercles each; moving towards the trailing edge, this number increases to a maximum of approximately 13 before decreasing to 6 or less. Tubercles of oblique ridges absent or indistinct, perhaps as a result of wear and/or abrasion.

The scapulocoracoids are more complete than those of *Gyracanthides murrayi* figured by Warren *et al.* (2000), though they are smaller in size. They have the same ridged bone texture and

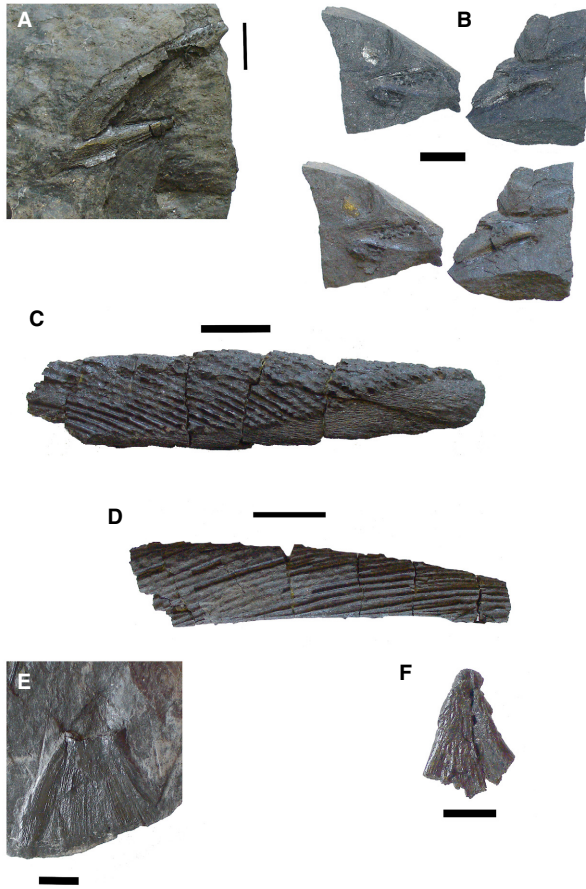


FIG. 4. Selected chondrichthyan bones. A, UMZC 2017.2.583, menaspiform holocephalan mandibular spine. B, UMZC 2017.2.526, menaspiform holocephalan mandibular spine in multiple views, with lighting changed to make morphology more easily visible. C, UMZC 2017.2.481, fin spine showing insertion area and tubercles on ridges. D, UMZC 2017.2.579, gyracanth spine showing ridges. E, UMZC 2017.2.582, partial scapulocoracoid. F, UMZC 2017.2.584, partial scapulocoracoid. All scale bars represent 1 cm. Colour online.

triangular shape, with the proximal portion showing a distinct tapering.

Remarks. Gyracanth spines are common in Devonian–Carboniferous non-marine settings (Turner *et al.* 2005; Snyder 2011). Turner *et al.* (2005) referred a number of Early Carboniferous records of *Gyracanthus* to *Gyracanthides*. However, both genera have been identified in Tournaisian collections from Blue Beach (Mansky & Lucas 2013). The two scapulocoracoids are identifiable as gyracanth on the basis of the presence of ridges and striae on both the internal and external surfaces (TRS pers. obs.) as well as their resemblance to the scapulocoracoids of *Gyracanthides* (Turner *et al.* 2005), though they are not diagnostic to the generic level. The gyracanth material is thus here only referred to Gyracanthidae indet.

Superorder HOLOCEPHALI Bonaparte, 1831
Order MENASPIFORMES? Obruchev, 1953 cf. Stahl 1999
MENASPIFORMES indet.

Figure 4A, B

Material. Two specimens, UMZC 2017.2.583 and UMZC 2017.2.526, each of one spine.

Diagnosis. Strongly asymmetric tuberculated dermal spine dividing into two major prongs, each subtriangular; larger, leading prong with prominent elliptic tubercles distributed distally, long axes oriented towards the probable leading edge.

Description. The leading spine is slightly convex along the presumed leading edge. The trailing spine is straight and subconical. The tuberculated surfaces are characteristic of menaspiform mandibular spines, most clearly described and depicted by Patterson (1965). The spines most closely resemble the mandibular spines of *Deltoptychius* (Patterson 1965, fig. 28C). However, they lack the spines on the distal tip. The broken area of UMZC 2017.2.583 is more completely preserved in UMZC 2017.2.526.

Remarks. Menaspiform holocephalans are a Permo–Carboniferous group known from, among other places, the Viséan of Scotland and Illinois (Stahl 1999). The taxonomy of the group is in need of revision. The specimens are not diagnostic to a lower level, and lack associated toothplates to aid identification. If they are correctly identified as menaspiform, they represent the earliest occurrence of the group.

Class OSTEICHTHYES Huxley, 1880
Subclass SARCOPTERYGII Romer, 1955
Order DIPNOI Müller, 1845
cf. *Uronemus splendens* Traquair, 1873

Figure 5A

Material. UMZC 2017.2.588, a single isolated tooth plate.

Diagnosis. Tooth plate with linearly arranged conical cusps, elongate ovoid base.

Description. UMZC 2017.2.588 is approximately 0.5 cm in length. There are three conical cusps arranged linearly along one side of an ovoid base.

Remarks. Specimen UMZC 2017.2.588 strongly resembles the vomerine tooth plate of *Uronemus splendens* as described and figured by Smith *et al.* (1987, fig. 20) in both size and morphology, differing chiefly in having three cusps per ridge instead of four. However, recent study of Tournaisian lungfish has found similar tooth plates in multiple taxa (TRS unpub. data), and it is not clear whether the marginal toothplates of *Uronemus* are unique or general.

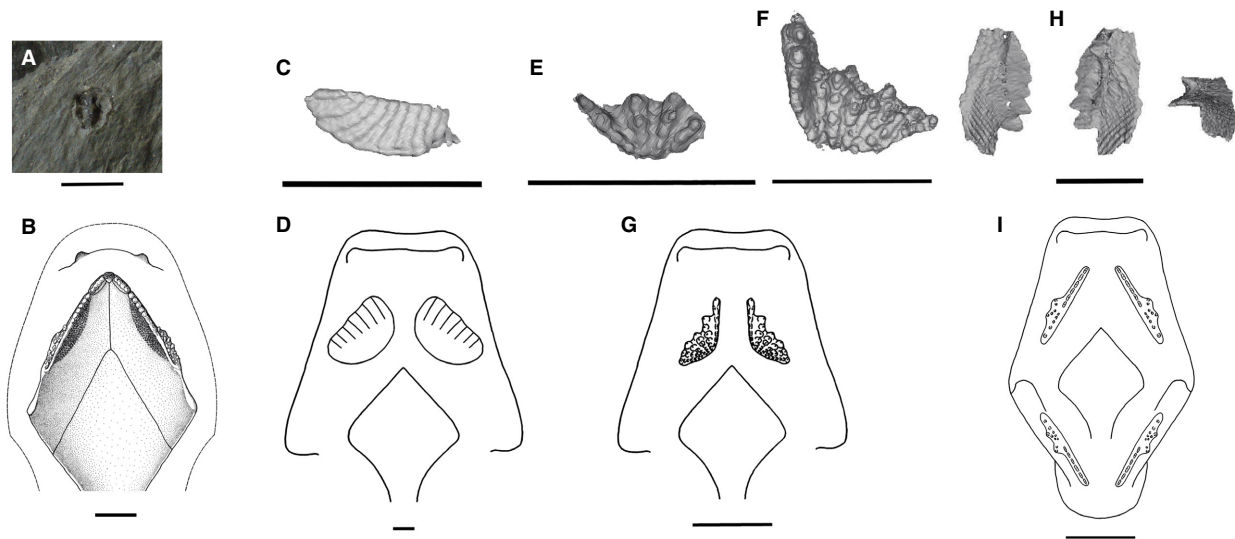


FIG. 5. Lungfish toothplates with reconstructions. A, UMZC 2017.2.588, vomerine toothplate resembling that of *Uronemus splendens*. B, reconstruction of *Uronemus* dorsal dentition modified from Smith *et al.* (1987). C, CT scan of toothplate assigned to *Ctenodus roberti*. D, reconstruction of *C. roberti* dorsal dentition from Smithson *et al.* (2015). E–F, CT scans of toothplates assigned to *Ballagadus caustrimi*. G, reconstruction of *B. caustrimi* dorsal dentition from Smithson *et al.* (2015). H, CT scan of partial toothplate assigned to *Xylognathus macrustenus* in multiple views. I, reconstruction of *X. macrustenus* dorsal and ventral dentition. CT scans are from UMZC 2015.46b. Scale bars represent: 1 cm (A, D, G, I); 0.8 cm (B); 0.5 cm (C, E, F, H).

cf. *Ctenodus roberti* Smithson *et al.*, 2015

Figure 5C

Material. A (partial?) pterygoid tooth plate only visible in CT scan from UMZC 2015.46b.

Diagnosis. Oval tooth plate with six tooth ridges without individual teeth.

Description. Oval-shaped tooth plate with six or seven slightly diverging tooth ridges lacking teeth. The tooth plate is flat, gently convex along the anterior edge and straight along the medial side. It is incomplete medially and posteriorly. Maximum length 4 mm; length to width ratio 3:1.

Remarks. This tooth plate resembles the holotype for *Ctenodus roberti* (Smithson *et al.* 2015, figs 3D, 4H). It is approximately seven times smaller than the *C. roberti* holotype. It is possible that it is incomplete laterally, but even allowing for this, it is much smaller than the *C. roberti* holotype.

cf. *Ballagadus caustrimi* Smithson *et al.*, 2015

Figures 5E–F, 6

Material. An incomplete skeleton represented by disarticulated cranial dermal bones, articulated ribs and fin ray supports

together with two (partial?) pterygoid tooth plates only visible in CT scan (Fig. 5E, F) from 2015.46b, and two sets of cranial dermal bones (Fig. 6A, B).

Diagnosis. Toothplate with four tooth ridges. More complete specimen (Fig. 5F) shows two teeth on the pterygoid ridge and four or five on the other ridges. Ridge angle approximately 100–120°.

Description. Both tooth plates are incomplete and appear to be lacking at least one tooth ridge. The largest specimen is *c.* 5 mm long, the other is 3 mm long. As preserved, the length to width ratio is *c.* 2.5:1. The largest specimen has four intact tooth ridges with the remains of a fifth. The smaller specimen has four partial tooth ridges. The tooth ridge angle on the largest specimen is *c.* 60° and *c.* 90° on the smaller specimen.

The skeleton (Fig. 6C–H) also appears to belong to *B. caustrimi*. The overall body length of the animal represented is approximately 8–9 cm, much smaller than *Ctenodus* spp. Fin supports are present dorsally and ventrally. Unlike *Xylognathus macrustenus*, the dorsal and anal fins do not seem to be separate. The head plates resemble those of a lungfish recovered from the surface of the palaeosol below the *Ossirarus* bed (Fig. 6A, B). While not much morphology is visible, the tail fin appears to be continuous dorsally and ventrally. The headplates are thick and subcircular, with very fine small tubercles.

Remarks. The tooth plates in the CT scan are similar to those of *Ballagadus caustrimi* (which is in turn highly

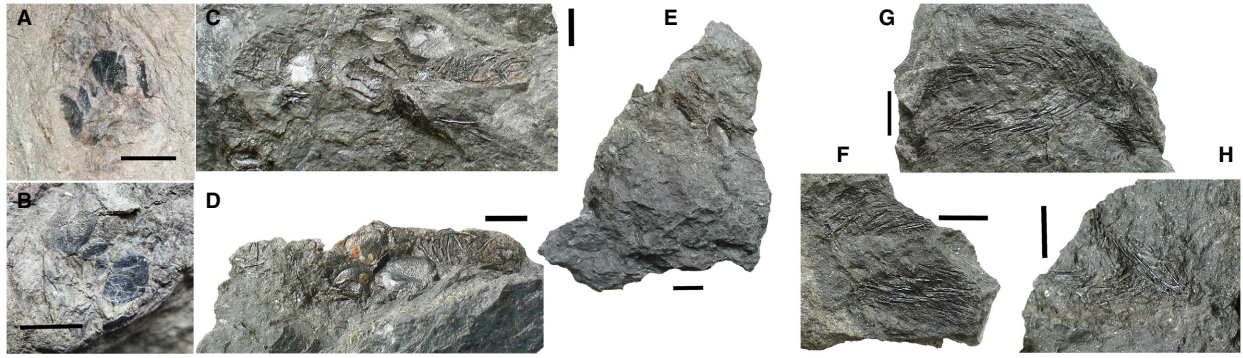


FIG. 6. Fossils attributed to *Ballagadus caustrimi*. A–B, uncatalogued skull bones from the *Ossirarus* bed. C–H, body fossils from the *Aytonerpeton* bed arranged anterior–posterior from C/D to G/H; C, E, G, UMZC 2015.46a, b, c; D, F, H: UMZC 2015.46d, c, e. All scale bars represent 1 cm. Colour online.

similar to *B. rossi*), particularly if they are assumed to be damaged. These tooth plates are half the size of the *B. caustrimi* tooth plate figured by Smithson *et al.* (2015), but are similar in size to those present on the referred specimen UMZC 2014.1.6a collected by Stan Wood (Smithson *et al.* 2015, p. 43). The skeleton (Fig. 6C–H) represents an animal with an overall length of approximately 8–9 cm, one of the smallest lungfish from the Ballagan Formation, and is probably similar in size to *Coccovedus celatus* (Smithson *et al.* 2015). Dorsoventral continuity of the tail fin has been considered characteristic of post-Devonian lungfish in contrast to Devonian forms, but has recently been recognized in Late Devonian lungfish (JAC pers. obs.).

cf. *Xylognathus macrustenus* Smithson *et al.*, 2015

Figure 5H

Material. The posterior portion of a pterygoid toothplate only visible in CT scan from UMZC 2015.46b.

Diagnosis. Narrow, flattened toothplate with two prominent teeth and (possibly) two more smaller teeth.

Description. This toothplate is clearly incomplete and corresponds to the posterior portion of the *Xylognathus* toothplate. It is flat and slightly curved along the long axis at an approximately 90° angle. Apart from damage/wear to the specimen, the surface appears to be smooth and lacking individual denticles.

Remarks. While the anterior portion of the toothplate is missing, the remaining posterior portion is a strong match for *Xylognathus*, particularly in preserving the distinctive two rows of teeth. It is also of comparable size to the pterygoid toothplate for *Xylognathus* as reconstructed by Smithson *et al.* (2015).

Order RHIZODONTIDA Andrews & Westoll, 1970
cf. *Strepsodus sauroides* Binney, 1841 *sensu* Jeffery 2006
Figure 7

Material. Incomplete and fragmentary skull bones, scales, a series of articulated vertebrae, numerous partial and complete cleithra and clavicles.

Diagnosis. Cleithrum with anastomosing ridged ornament. Clavicle with tuberculate ornament and rounded anterior tip. Simple, cylindrical vertebrae. Subcircular scales with ridged exterior surface and central boss in internal view.

Description. Cleithra range from almost complete specimens to fragments. When preserved on the cleithra, the dorsal laminae all have a slight ridge running down the external ascending blade with a slight prominence at the top (Z. Johanson pers. comm. November 2017). This differentiates the cleithrum of *Strepsodus* from the cleithrum of *Screbinodus* (Andrews 1985).

The vertebrae are articulated and exposed in probable ventral or ventrolateral view. The vertebrae (Fig. 7A) are smooth, massive, and broad-waisted. They are extremely similar to the *Strepsodus* vertebrae figured by Andrews & Westoll (1970, pl. 13a). This morphology contrasts with the more pleisiomorphic rha-chitimus vertebrae of more basal rhizodonts such as *Barameda* (Garvey *et al.* 2005), and they are much more robust than those of *Hongyu* (Zhu *et al.* 2017).

Remarks. While rhizodont cleithra are often preserved due to their robustness, even in juveniles (Andrews & Westoll 1970; Andrews 1985; Davis *et al.* 2001), they are highly variable within species due to age and individual variation. The dermal bone fragments are united in having either a tuberculate or ridged ornament. The quality of the preservation of the ornament varies but the ornamentation patterns are consistent. This suggests that the varied material can be assigned to *Strepsodus* despite its being isolated.

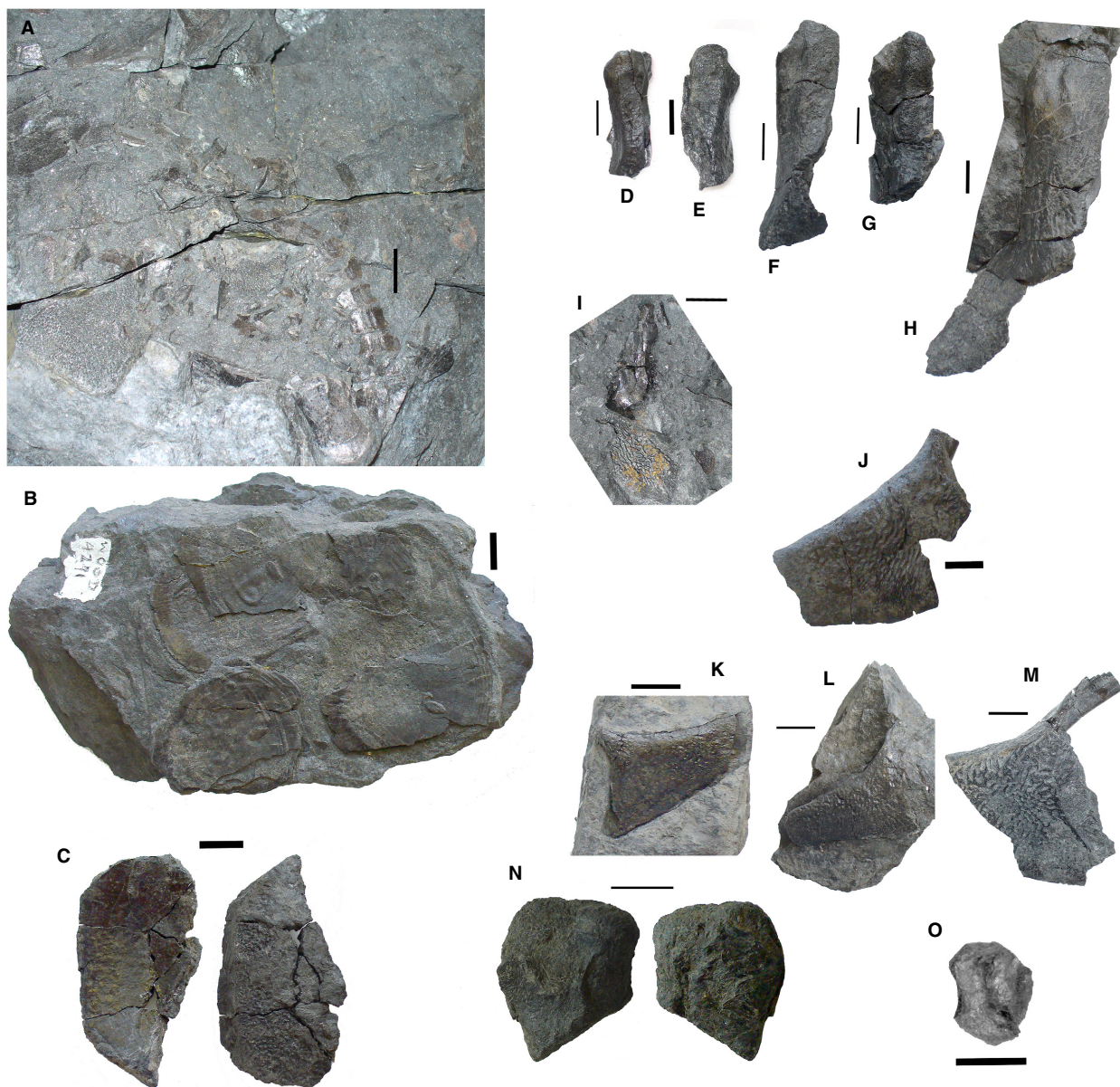


FIG. 7. Various rhizodont bones assigned to *Strepsodus*. A, UMZC 2017.2.578, vertebrae in articulation. B, UMZC 2017.2.520, scales. C, UMZC 2017.2.447, opercular or subopercular in internal and external views. D–H, cleithra showing growth series: D, UMZC 2017.2.537; E, UMZC 2017.2.541; F, UMZC 2017.2.571; G, UMZC 2017.2.539; H, UMZC 2017.2.515a. I, UMZC 2017.2.672, smallest cleithrum in internal view. J, UMZC 2017.2.534, partial left clavicle showing dermal ornament. K, UMZC 2017.2.535 partial right clavicle. L, UMZC 2017.2.531, partial left clavicle. M, UMZC 2017.2.532, partial left clavicle. N, UMZC 2017.2.538, partial humeral head. O, UMZC 2017.2.538, radius. All scale bars represent 1 cm. Colour online.

aff. *Archichthys portlocki* sensu Jeffery, 2006

Figure 8

Possible synonyms. ‘cf. *Archichthys portlocki*’, GLAHM 152115, GLAHM 152121, GLAHM 152252 (Carpenter *et al.* 2014); ‘*Archichthys portlocki*’ YPM VPPU 019334, NSM008GF040.063 (Carpenter *et al.* 2015); ‘*Archichthys portlocki*’ NBMG 15799, 15818, 19972 (Ó Gogáin *et al.* 2016).

Material. UMZC 2017.2.465 and UMZC 2017.2.458 from Burnmouth, UMZC 2017.2.551 and UMZC 2017.12.2 from Coldstream.

Diagnosis. Recurved, robust teeth with short, anastomosing striae. Striae form a ‘collar’ around the circumference of the tooth and are absent from the tip. Twelve basal plications.

Description. The teeth include both isolated singletons, teeth attached to jaw fragments, and a possible vomer, UMZC

FIG. 8. Rhizodont teeth showing unusual striation pattern. A–B, UMZC 2017.2.465, vomer with tooth in: A, medial; B, occlusal view. C, UMZC 2017.2.465, enlarged view of tooth showing striation pattern. D, UMZC 2017.2.458, teeth in ?medial view showing striation pattern. E–F, UMZC 2017.2.551, tooth from Bed 1 at Burnmouth, 383 m in the section (approximately 45 m above the TIM). G–H, UMZC 2017.12.2, tooth from the Coldstream locality showing striation pattern. Scale bars represent: 1 cm (A, B, E–H); 0.5 cm (C, D). Colour online.



2017.2.458. UMZC 2017.2.458 is heavily damaged, but the bone is approximately teardrop-shaped in occlusal view. A wall of bone brackets approximately half the circumference of the tooth and extends straight posteriorly.

The teeth are circular to oval in cross-section. Where preserved, the bases appear to have 12 plications. The teeth vary in size, suggesting that the striation pattern is present on teeth across the jaw. None of the teeth preserve the sigmoid tip characteristic of *Strepodus* dentary fangs. Apart from the striation pattern they are otherwise like the teeth of *Archichthys*, robust as opposed to the slender teeth of *Letognathus* which share a similar striation pattern (Brazeau 2005). The presence of striae distinguishes them from the smooth teeth of *Rhizodus* and *Screbinodus* (Andrews 1985).

The striation pattern differs from that of *Strepodus*, which is composed of larger parallel striae (Jeffery 2006).

Remarks. These teeth are difficult to distinguish from those of *Archichthys* given the similarity in striation pattern, and teeth from the Ballagan on the Isle of Bute have been assigned to *Archichthys* previously (Carpenter *et al.* 2014). The situation is not helped by the current limits of reliably-assigned *Archichthys* material (Jeffery 2006). However, the presence of these teeth in the TIM, elsewhere at Burnmouth, and at Coldstream, another Ballagan locality (see Smithson *et al.* 2012 for more

locality information) suggests that genuine variation is being sampled. Given the confounding effects of tooth and scale taxonomy on our understanding of rhizodonts (Andrews 1985; Jeffery 2006) and the state of ongoing work, we are hesitant to erect a new taxon at this time.

Superclass TETRAPODA Goodrich, 1930

aff. *Pederpes* Clack, 2002 and *Whatcheeria* Lombard & Bolt, 1995

Material. UMZC 2016.8, two incomplete possible frontal and prefrontal bones, possibly with partial nasal (Fig. 9A, B; Clack *et al.* 2016, fig. 6F, G), UMZC 2017.2.569, a cleithrum (Fig. 9C), UMZC 2016.9, partial maxilla with teeth (Fig. 9D), UMZC 2017.2.611, a radius (Fig. 9E), digit bones (e.g. UMZC 2017.2.577, Fig. 9F), and UMZC 2017.3.576, an intercentrum (Fig. 9G).

Diagnosis. Ornament on skull roof bones subcircular at the centre of the bone and more ovoid toward the

margin. Teeth anteroposteriorly compressed in cross-section. Maxilla and cleithrum with fine ornament texture.

Description. The ornament of the frontals contrasts with that of *Pederpes*, which has a pattern of pits with ridges and grooves; ornament in *Whatcheeria* is limited to very light pitting. The proportions of the bones suggest suggest that they are more similar to the relatively short and narrow frontals of *Whatcheeria* and *Pederpes* than the longer frontals of *Greererpeton*. The shape of the right frontal implies a broad, triangular prefrontal as in *Whatcheeria*.

The stem of the cleithrum is narrow and straight, more similar to that of *Whatcheeria* than *Pederpes*. However, the dorsal expansion, though incomplete, does not seem to have the characteristic notch of *Whatcheeria*. Among the jaw material (Fig. 9D), there is both a ‘large’ size fraction (approximately 9 cm) and a ‘small’ size fraction (approximately 1 cm). However, all of these preserve teeth with the same anteroposteriorly compressed cross-section. The toe bones are longer than broad, are clearly waisted, asymmetrical, and strongly concave on the flexor surface. In this they resemble the proximal foot bones of

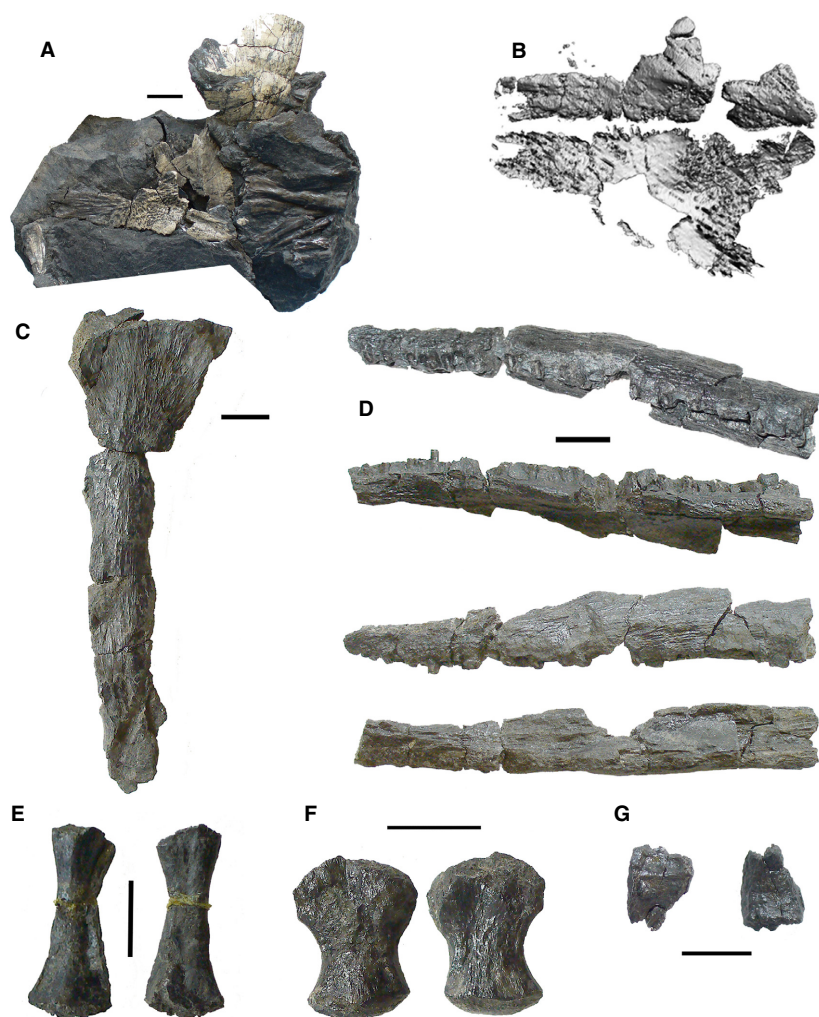


FIG. 9. Selection of TIM ‘whatcheeriid’ material. A–B, UMZC 2016.8, paired frontals; B, CT scan; the lower frontal is exposed in the specimen. C, UMZC2017.2.569, cleithrum. D, UMZC 2016.9, left maxilla in multiple views. E, UMZC 2017.2.611, radius in external and internal view. F, UMZC 2017.2.577, digit in dorsal and ventral view. G, UMZC 2017.3.576, intercentrum in external (left) and internal (right) views. All scale bars represent 1 cm. Colour online.

Pederpes but contrast with those of *Whatcheeria*, which are much flatter and broader than long (BKAO pers. obs.)

Remarks. The skull bones are most like those of *Pederpes* and *Whatcheeria*. However, confirmation must await more complete specimens. The other specimens are not associated with the skull bones, but resemble *Whatcheeria*/*Pederpes* in some respects, contrast with the colosteid-like morphology of *Aytonerpeton* and are too large to be assigned to *Diploradus*. The jaw material is particularly interesting; the distinctive tooth morphology seems to be unique and allows for the unification of specimens of multiple sizes. UMZC 2014.14, a maxilla collected from Heads of Ayr by JAC in 2014 (see Clack *et al.* 2016, suppl. data), appears to have a similar tooth morphology. Though there is not sufficient material for a formal diagnosis, we suspect this represents a new taxon.

cf. *Aytonerpeton microps* Otoo, Clack & Smithson
in Clack *et al.*, 2016
Figure 10

Material. UMZC 2016.7, a partial skull table, and UMZC 2016.6b, a parasphenoid.

Diagnosis. Tetrapod skull table with colosteid-type dermal ornament, curved posterior orbital margin, and circular parietal opening without thickened margin. Parasphenoid with short dorsum sellae and extensively denticulated posterior plate.

Description. The skull table is exposed in internal view (Fig. 10A). The pattern of dermal ornament is extremely similar to that of *Aytonerpeton*, if not identical. Exposures of the lateral line are visible on the postfrontals and postorbital. The pattern

of lateral line exposure is nearly identical to that of *Greererpeton* in the same region (Smithson 1982). The parietal opening is relatively much larger.

A lower-resolution image of the parasphenoid was included in the supplement to Clack *et al.* (2016). In Figure 10D–H the sculpturing on the ventral surface of the cultriform process and denticulation on the posterior plate are more clearly visible. Clack *et al.* (2016) pointed out the short dorsum sellae, comparing it to later temnospondyls, as well as noting the unique extent of posterior plate denticulation. The morphology of the parasphenoid contrasts strongly with that of *Greererpeton*, having a broader posterior plate and a relatively shorter, broader cultriform process. This is suggestive of a broader, less elongate skull.

Remarks. The size of both the parasphenoid and skull table are consistent with them belonging to *Aytonerpeton*. The proportions of the parasphenoid are consistent with the skull proportions of *Aytonerpeton*, which has a much shorter skull than *Greererpeton*. The colosteid-like lateral line exposure on the skull roof and the great similarity in dermal ornament to *Aytonerpeton* suggest that it belongs to that taxon. However, definitive assignment must await the discovery of more complete *Aytonerpeton* specimens against which these can be compared.

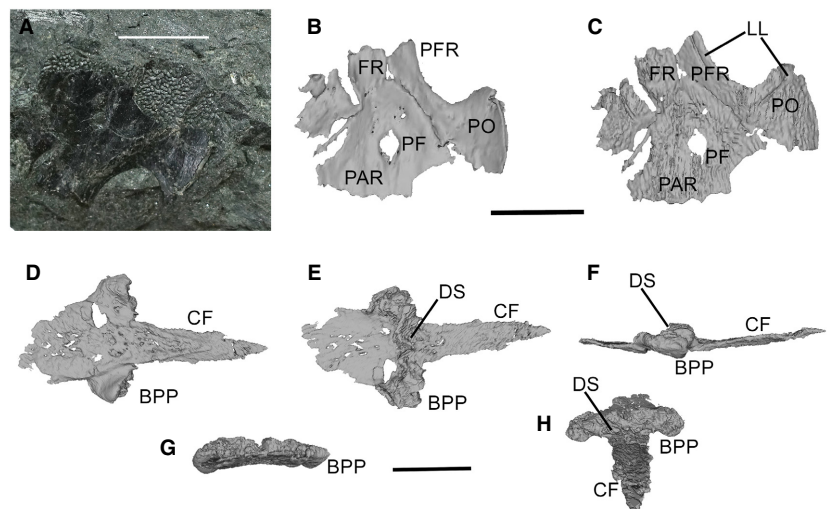
Class ACTINOPTERYGII Cope, 1887
ACTINOPTERYGII indet.

Figure 11

Material. Isolated scales (e.g. UMZC 2017.2.719 and UMZC 2017.2.718, Fig. 11B, C), rarer squamation (Fig. 11A), UMZC 2017.2.717, an isolated dermal bone (Fig. 11D), and UMZC 2017.2.668, a partial skull roof (Fig. 11E).

Diagnosis. Ornament-covered scales with either diamond shape or elongate trapezoidal shape. Diamond-shaped

FIG. 10. Tetrapod material cf. *Aytonerpeton*. A, UMZC 2016.7, skull table exposed in interior view with mould of dermal ornament. B–C, CT scan of the same specimen in: B, external; C, internal view. D–F, UMZC 2016.6b, parasphenoid in: D, ventral; E, dorsal; F, right lateral; G, posterior; H, antero-dorsal view. **Abbreviations:** BPP, basiptyergoid process; CF, cultriform process; DS, dorsum sellae; FR, frontal; LL, lateral line; PAR, parietal; PF, pineal foramen; PFR, postfrontal; PO, postorbital. All scale bars represent 1 cm.



scales have anterodorsal process and dorsal peg. Dermal bones ornamented with either smooth elongate tubercles or ridges.

Description. Two different actinopterygian scale morphologies are present: smaller, more equidimensional scales that occur as hash (Fig. 11A) and larger, dorsoventrally elongate scales that are found in isolation (Fig. 11B, C). The former are shiny, whereas specimens of the latter exhibit variable amounts of lustre. The morphology of the smaller scales is consistent with their being from the caudal lobe of the tail; the larger scales probably come from the flank.

UMZC 2017.2.717 appears to come from the roof of the skull. It is possible that instead of being a single bone it is a set of paired bones. UMZC 2017.2.668 is a partial skull roof, encompassing parts of the frontals and parietals. The ridged ornament pattern is common to many early actinopterygian genera (Daeschler 2000; Friedman & Blom 2006; Mickle 2011, 2017; Sallan & Coates 2013). The orbital margin is long. The frontals are more than twice as long as the parietals and incomplete anteriorly. The posterior margin of the parietals is indented at the midline. The growth centre of the right frontal is visible, marked by the central whorl of ornament. The pits of the supraorbital canal are also discernable, crossing over the centre of the right frontal and curving laterally near the parietal. The right parietal shows the three pit lines characteristic of actinopterygians.

Remarks. Though there are actinopterygian fossils present in numerous samples from the TIM, in absolute terms the amount of material is small and mostly consists of scales. The proportions of the frontals and parietals compares favourably with that of *Limnomis* (Daeschler 2000) and *Cuneognathus* (Friedman & Blom 2006) from the Famennian, both of which are small-bodied. However, they contrast with *Avonichthys* from the Tournaisian (Wilson *et al.* 2018). Interestingly, the elongation of the frontals relative to the parietals has been considered a derived character. None of the taxa appear to have an indented posterior parietal margin, but such an indent appears in *Rhabdolepis macropterus* from the Permian (Schindler 2018).

The phylogenetic analysis of Friedman & Blom (2006) recovered *Limnomis* and *Cuneognathus* as the sister taxa to *Kentuckia* from the Visean. While there is not enough material for a phylogenetic analysis or taxonomic assignment, the morphology of UMZC 2017.2.668 suggests that it may be part of this Devonian–Carboniferous group.

RESULTS

Sedimentology results

The fossil-rich interval represents a change in sedimentary environment from permanently wet and marshy

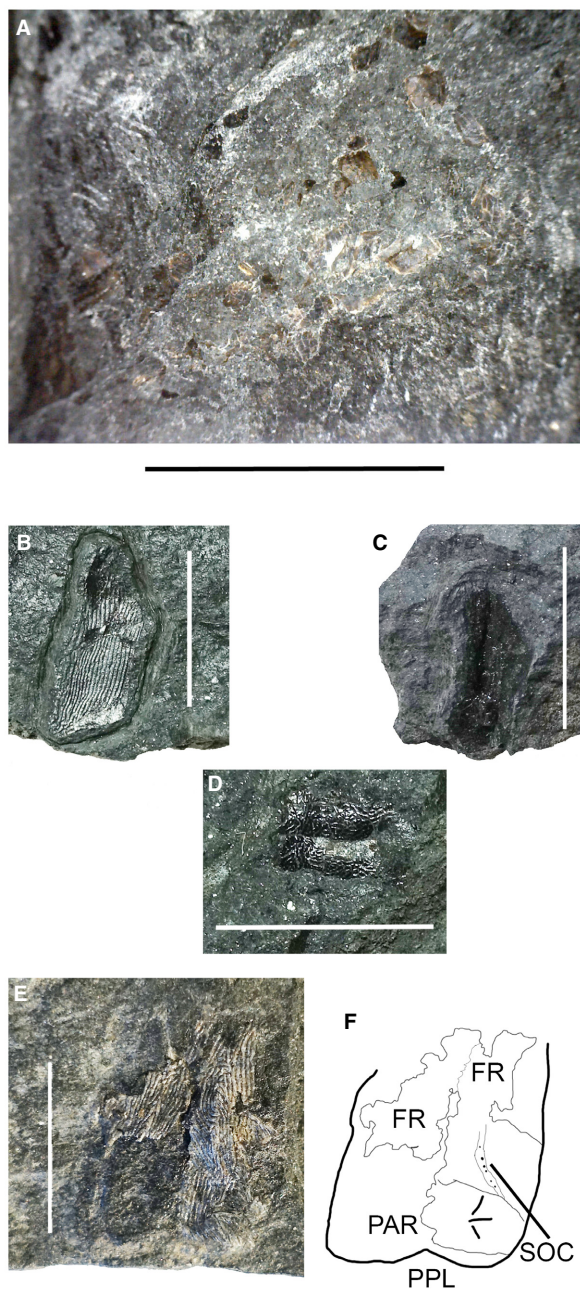


FIG. 11. Overview of actinopterygian material. A, scale hash from 2015.46. B, UMZC 2017.2.719, isolated scale. C, UMZC 2017.2.718, isolated scale. D, UMZC 2017.2.717, dermal bone(s). E–F, UMZC 2017.2.668, partial skull roof, anterior is at the top of the image; F, interpretive drawing at same scale. *Abbreviations:* FR, frontal; PAR, parietal; PPL, parietal pit lines; SOC, supraorbital canal. All scale bars represent 1 cm.

conditions to seasonally wet conditions (Clack *et al.* 2016). The 250 cm thick section that contains the TIM illustrates this transition in detail (Fig. 2). The lower half of the section (up to 1.4 m height) includes a dolostone bed at the base, which contains ostracods and fish debris

and has a brecciated top. This is overlain by a sequence of two 40–50 cm-thick gleyed inceptisols (cf. Kearsy *et al.* 2016), interbedded with mottled siltstones and sandy siltstones. Desiccation cracks occur in three horizons and are infilled with sandy siltstone. Dolostone nodules are associated with the lower gleyed inceptisol but are localized, and only present on the foreshore. The upper half of the section contains a complex sequence of fossil-rich sandy siltstones (Fig. 2, Detailed Log). Overlying this is a sequence of interbedded laminated grey siltstones and red siltstones (inceptisols), which have numerous desiccation cracks. At the top of the section a vertisol red siltstone bed contains green drab root haloes. For full description of palaeosol facies, see Kearsy *et al.* (2016).

The detailed log illustrates the complexity of the fossil-rich interval (Fig. 2). At the base is a thin gleyed Inceptisol, the top of which is brecciated and infilled by the overlying sandy siltstone. In thin section this bed is light grey, mottled, with fish scales, plant and ostracod fragments at random orientations within a coarse siltstone matrix (Fig. 3, thin section 1). The top of the gleyed inceptisol has an irregular surface, attributed to erosion by the overlying sandy siltstone bed (Fig. 3A). This sandy siltstone bed is laterally variable in thickness and in the metre-square section it has desiccation cracks in the centre and at the top (Fig. 2) indicating that it is a composite of two event beds (Fig. 12). This is overlain by a thin laminated grey siltstone bed which is localized to the foreshore (not present in the cliff exposure). Above this is the first tetrapod-bearing bed, containing *Ossirarus*, an organic-rich, structureless, black sandy siltstone (Fig. 3A, B). Overlying this dark sandy siltstone bed are two very fine sandstone beds, with asymmetric ripple lamination, that fine upwards into siltstone. Their thickness on the foreshore is 2–4 cm, with thinner beds observed in the cliff section (Figs 2, 3).

The second tetrapod-bearing bed, with *Aytonerpeton*, is a 9 cm, structureless, dark grey sandy siltstone. In thin-section this bed is characterized by a fine-grained siltstone matrix with sub-millimetre sized clasts of siltstone, sandstone and bioclasts (Fig. 3, thin section 2), while in the metre-square section, larger light green siltstone clasts up to 5 mm in size are present, which are of a similar lithology to the underlying gleyed inceptisol. Plant material is abundant and plant fossils are sometimes flow-aligned to produce a wavy fabric. Overlying this bed is a sequence of laminated grey siltstone, with millimetre-thick sandstone lenses. Within this bed is a thin sandy siltstone inter-bed that infills desiccation cracks (Fig. 3, thin section 3). Above the laminated bed is another sandy siltstone, containing a green siltstone lens, which is the last sandy siltstone in the sequence. At the top of the detailed log sequence are further laminated grey siltstones, with sparse desiccation cracks.

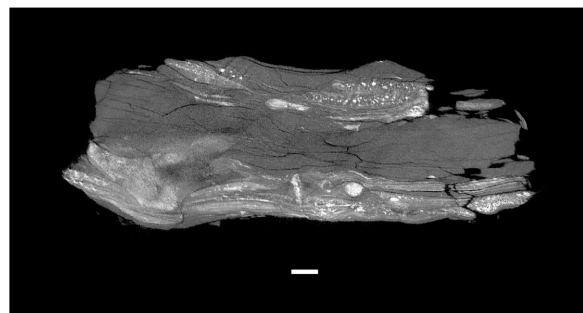


FIG. 12. CT scan of UMZC 2017.2.483 before preparation, showing the internal stratigraphy of the fossil-rich layer captured by the TIM. This specimen does not come from within the TIM itself but was laterally adjacent to it. Note the two event beds marked by the fossil concentrations at the top and bottom of the specimen. Scale bar represents 1 cm.

Microfossil results

The purpose of this microfossil study is to characterize the microfossil assemblages in terms of palaeoenvironments, not to describe the taxonomy of fossil specimens. Each sample has a unique microfossil assemblage (Fig. 13). Microfossils are generally well preserved, with minimal wear, abrasion, or cracks observed.

Sample 1: palaeosol. The assemblage is dominated by ostracods, with a minor component of actinopterygian scales, one actinopterygian tooth, one rhizodont scale and plant fragments (Fig. 13). The majority of ostracods present are poorly preserved; the following were identified to genus level: *Beyrichiopsis*, *Cavellina*, *Glyptolichvinella*, *Paraparchites*, *Shemonaella*, *Silenites*, *Sulcella* (Fig. 14A–D). This assemblage is typical of the fine-grained clastic lithologies of the Ballagan Formation (Williams *et al.* 2005). Of these, *Cavellina*, *Shemonaella* and *Glyptolichvinella* are most numerous within the sample (Otoo *et al.* 2018, micropalaeontology data). The 1 mm and 425 μm fractions have a ratio 1:3 carapaces:single valves, while the 250 and 125 μm fractions contain mostly broken single valves, which is probably an artefact resulting from breakage during sieving. Ostracod juveniles with the full instar size range are present and there is no apparent size sorting of the assemblage. The actinopterygian tooth (Fig. 14E) lacks the apical cap but preserves the characteristic cross-hatched surface texture (Carpenter *et al.* 2011).

Sample 2: sandy siltstone. This sample has the highest number of fossil specimens, at 98.7 fossils/g, which is twice as many as sample 1 and five times more than sample 3 (Otoo *et al.* 2018, micropalaeontology data). The assemblage is dominated by plant material (fibrous fragments, probably from plant stems) and rhizodont scale

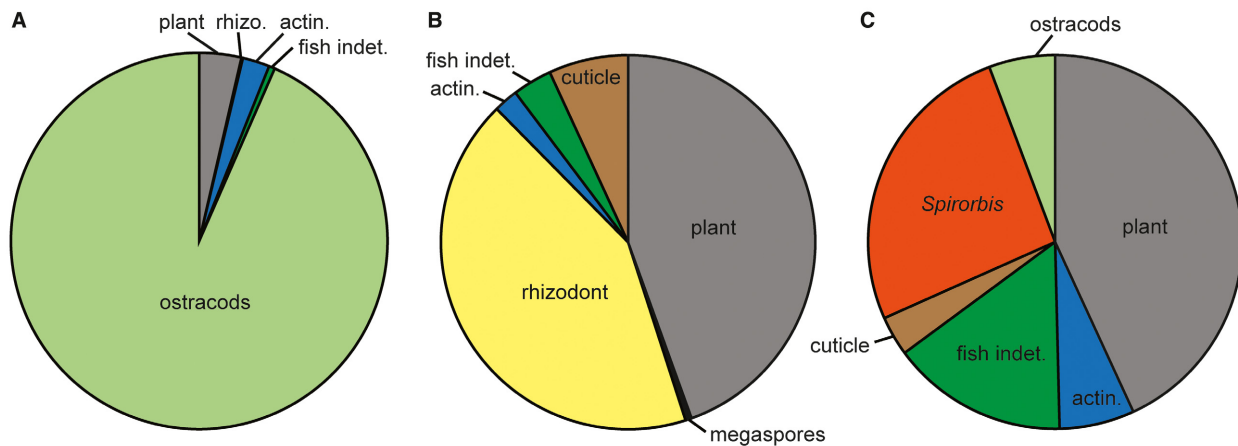


FIG. 13. Microfossil assemblages. Percentage counts of total assemblage microfossil counts for three samples. A, sample 1 (palaeosol, $n = 777$ specimens). B, sample 2 (sandy siltstone, $n = 1470$). C, sample 3 (laminated grey siltstone, $n = 262$). The full data table of counts for all size fractions and microfossils per gramme is presented in Otoo *et al.* (2018). Abbreviations: actin., actinopterygian; indet., indeterminate; rhizo., rhizodont. Colour online.

and bone fragments (Fig. 13). Rhizodonts are also dominant in the underlying *Ossirarus* bed that was sieved and picked for microfossils as a pilot study, but not quantitatively picked (Fig. 14F–H). The exterior surface of the scales has a fibrous structure, and shiny, silver colour. When broken, the interior layers have a range of structural elements characteristic of rhizodonts (Andrews 1985) including sheets of either tubercles and pits or grooves and ridges that interlock together. These structures were identified by the examination of broken rhizodont scale macrofossils from the TIM interval. Also present are indeterminate megaspores (with a smooth external surface, no visible trilete marks; Fig. 14I), actinopterygian scales and teeth. Actinopterygian scales have a rhombic shape with a smooth interior surface with keel, and sculpted exterior surface with transverse ridges or grooves (Fig. 14J–K). Small rows of curved unornamented actinopterygian teeth, probably pharyngeal in origin, occur solely within the 125 μm fraction (Fig. 14M–N). Indeterminate brown or black cuticle occurs within all size fractions, and in sample 3. One fragment of semi-lunate shaped eurypterid scale occurs in the underlying *Ossirarus* sandy siltstone bed (Fig. 14L). Dipnoan and tetrapod microfossils have not been recorded from this bed,

because of the difficulties of scale and bone fragment identification and their relative rarity compared to the other vertebrates. The amount of unidentified vertebrate bone and scale material varies per sample (sample 1: 0.5%; sample 2: 3.4%; sample 3: 15.2%; Otoo *et al.* 2018, micropalaeontology data).

Sample 3: laminated grey siltstone. The sample has a lower number of specimens in each size fraction compared to the other two samples. Plant fragments, *Spirorbis* and actinopterygian bone and scale fragments dominate the assemblage (Fig. 13). *Spirorbis* specimens are fragmented and pyritized (Fig. 14O). Ostracod fragments, indeterminate cuticle and one rhizodont scale fragment are also present. The 125 μm fraction contains a higher number of actinopterygian fragments than the other size fractions, consisting of small scale and bone debris.

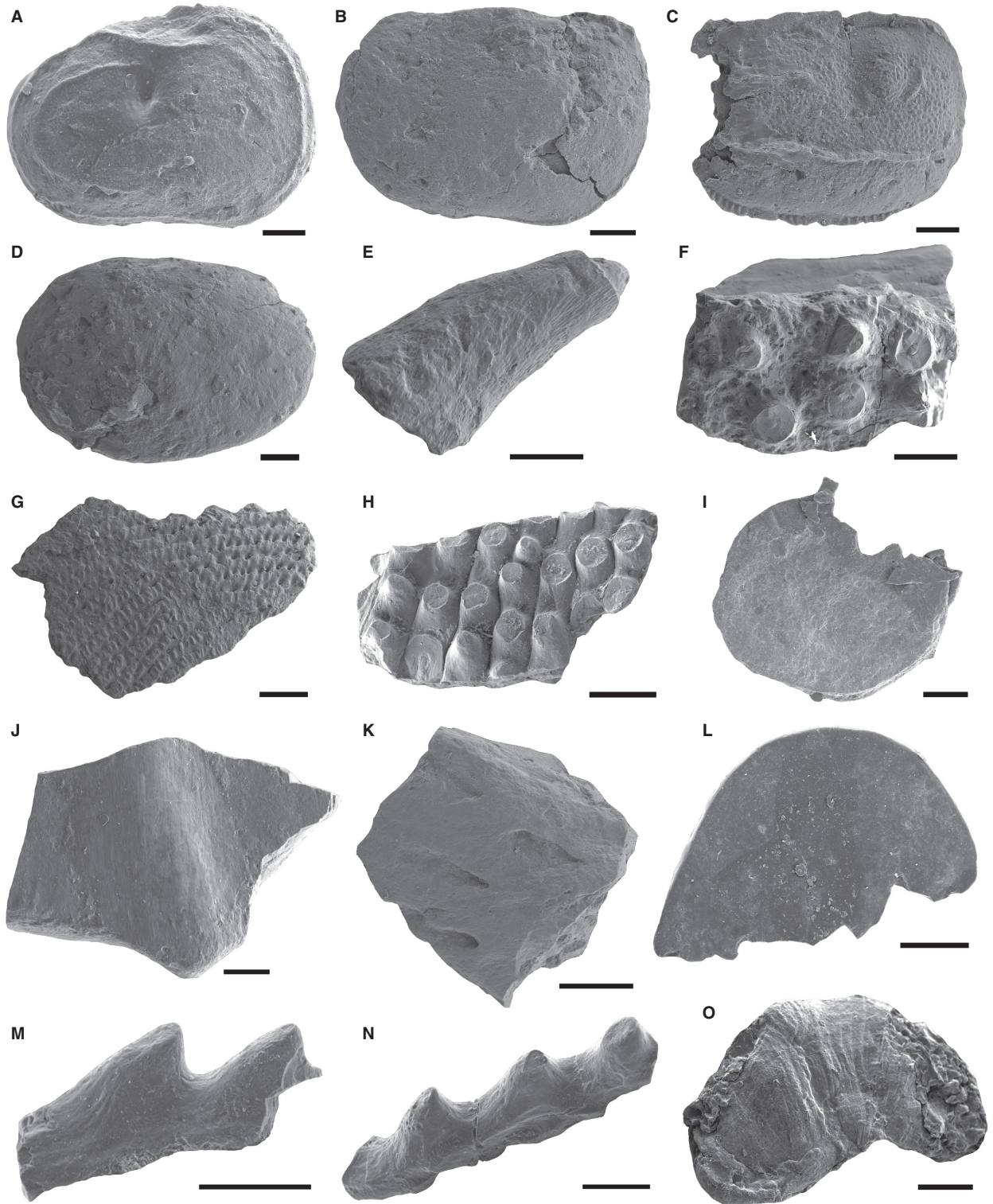
Faunal similarity analyses

In all analyses, Devonian and Carboniferous localities plot on opposite sides of the origin along the x -axis (Figs 15–18). The convex hulls for each stage overlap within their

FIG. 14. Selected microfossil specimens. A, *Glyptolichvinella*, juvenile, left valve, partially broken, lateral view, microfossil sample 1. B, *Shemonaella*, juvenile, left valve, lateral view, microfossil sample 1. C, *Beyrichiopsis*, adult, left valve, lateral view, broken specimen with a single costa, microfossil sample 1. D, *Cavellina*, adult, carapace, right lateral view, microfossil sample 1. E, actinopterygian tooth, broken cap, lateral view, microfossil sample 1. F, rhizodont dermal bone, view of the exterior surface with pustular ornamentation, from the *Ossirarus* sandy siltstone bed. G–H, rhizodont scales, with two different internal structures, *Ossirarus* bed. I, megaspore, indeterminate, with smooth external surface, broken specimen, microfossil sample 2. J–K, actinopterygian scale fragments, microfossil sample 2: J, interior; K, exterior surfaces. L, single scale, broken, from eurypterid cuticle, *Ossirarus* bed. M–N, pharyngeal actinopterygian teeth, lateral view, microfossil sample 2. O, pyritized *Spirorbis* tube fragment, microfossil sample 3. Scale bars represent: 100 μm (A–E, J, M, N); 500 μm (F, G); 250 μm (H, I, K, L, O).

respective period, but there is no Devonian/Carboniferous overlap. Attempted analyses using environmental sub-categories proved unsuitable within the constraints of the methods used here and are not included.

Correspondence analysis. When the total dataset is analysed using correspondence analysis (CA), marine sites generally plot below 0 on the *y*-axis and non-marine (= marginal + continental) sites plot above 0 (Fig. 15).



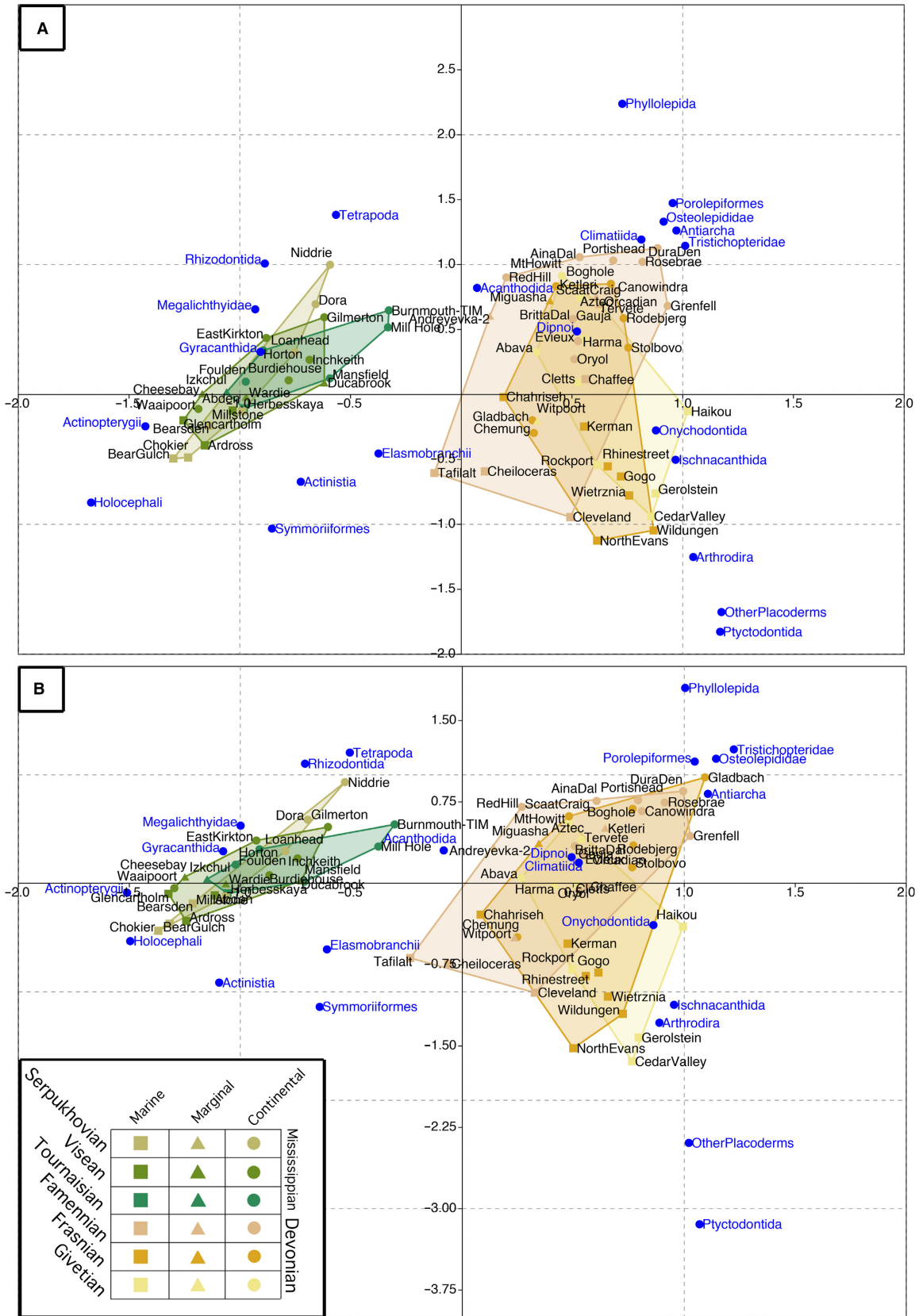


FIG. 15. Correspondence analysis results, full dataset. A, raw diversity. B, relative diversity.

Thus four broad time-setting associations emerge when the entire raw diversity dataset (Fig. 15A) is analysed:

1. Devonian marine: Onychodontida, Ischnacanthida, Arthrodira, Ptyctodontida, other placoderms.
2. Devonian non-marine: Phyllolepada, Dipnoi, Acanthodida, Climaatiida, Porolepiformes, Osteolepididae, Antiarcha, Tristichopteridae.
3. Carboniferous marine: Elasmobranchii, Actinistia, Symmoriiformes, Holocephali, Actinopterygii.
4. Carboniferous non-marine: Tetrapoda, Rhizodontida, Megalichthyidae, Gyraacanthida.

Analysis of the entire relative diversity dataset returns the same broad associations, except acanthodians move to the Carboniferous non-marine association (Fig. 15B). In both the raw and relative diversity analyses Burnmouth-TIM emerges closest to Mill Hole (Fig. 15).

When only the non-marine sites are analysed, marginal sites do not plot separately from continental sites in any recognizable pattern, though the relative Devonian/Carboniferous positions are maintained (Fig. 16). The Givetian convex hull overlaps less with the Frasnian and Famennian hulls, and the Serpukhovian hull no longer overlaps with the Tournaisian and Visean hulls. Burnmouth-TIM plots roughly equidistant from Mill Hole, Gilmerton, and Niddrie. When raw diversity (Fig. 16A) is analysed the following associations are recovered:

- Devonian: Climaatiida, Onychodontida, Acanthodida, Ptyctodontida, Ischnacanthida, Osteolepididae, Arthrodira, Phyllolepada, Actinistia, other placoderms.
- Devonian: Dipnoi, Antaircha, Porolepiformes, Tristichopteridae, Phyllolepada.
- Carboniferous: Actinopterygii, Megalichthyidae, Symmoriiformes, Elasmobranchi.
- Carboniferous: Tetrapoda, Rhizodontida, Gyraacanthida, Holocephali.

When relative diversity is analysed (Fig. 16B), actinistians join the actinopterygian-megalichthyid-elasmobranch-symmoriiform association, and phyllolepids join the other Devonian association.

Non-parametric multidimensional scaling. As with the correspondence analysis results, in the NMDS results Devonian and Carboniferous sites are separated along the *x*-axis (co-ordinate 2) and marine and non-marine sites are separate along the *y*-axis (co-ordinate 1; Fig. 17). The relative positions of the individual sites are similar to those in the correspondence analysis (CA) results. In analyses of both the total raw diversity dataset (Fig. 17A) and the total relative diversity dataset (Fig. 17B), Burnmouth-TIM emerges closest to Mill Hole and nearby Gilmerton, Niddrie and Dora. When only non-marine sites are analysed (Fig. 18), as with the CA results the overlap between the Givetian and Serpukhovian hulls and those of the other Devonian and Carboniferous stages,

respectively, decreases, more so for raw (Fig. 18A) than relative diversity (Fig. 18B). Burnmouth-TIM maintains its relative position.

DISCUSSION

Sedimentology interpretation

The depositional environments represented in the 250 cm-thick section (Fig. 2) are diverse. The basal dolostone represents deposition in a saline-alkaline lake, with a marine influx onto the floodplain attributed to storm activity (Bennett *et al.* 2017). The mottled grey siltstones and green palaeosols represent deposition within a floodplain lake, then the growth of vegetation. Although periods of desiccation occurred in the lower part of the section, in general the soils were waterlogged and the environment was probably a saline (brackish) marsh (Kearsey *et al.* 2016). Sandy siltstones were deposited as cohesive debris flows in flooding events after periods of desiccation (Bennett *et al.* 2016). In the 40 cm-thick fossil-rich interval numerous flooding events deposited a sequence of six sandy siltstone beds, some of which overlie desiccation cracks. Lateral variability in the thickness and internal structure of sandy siltstones and very fine sandstones between the cliff and foreshore exposures highlight the localized origin of these deposits.

A modern analogue for the dry/wet alternations seen in the palaeosol/sandy siltstone association are mud aggregates in dryland river floodplains (Rust & Nanson 1989; Wakelin-King & Webb 2007a, b). However, the climate of the Ballagan Formation is interpreted as tropical, with seasonal monsoonal rainfall (Falcon-Lang 1999; Kearsey *et al.* 2016). Sandy siltstone deposits have not been reported from other sites in the geological record, and have probably been reported as massive siltstone beds, due to the small size of their clasts. However, a similar facies occurs in the Early Cretaceous Wessex Formation, Isle of Wight. Here plant debris beds contain a similar fauna and are also interpreted to have formed as debris flow deposits during flooding events in a tropical climate (Sweetman & Insole 2010). These plant debris beds infill local depressions on the floodplain and also contain sediment clasts and fossils within a siltstone matrix. They differ from sandy siltstones in having larger-sized clasts and fossils (including dinosaur bones) but are otherwise interpreted to have formed by a similar mechanism. Overbank deposits preserve tetrapod fossils at the Famennian site of Red Hill, Pennsylvania, but further study is needed to determine whether the standing water taphofacies described as 'green-grey siltstones with abundant plant material and an occasional occurrence of arthropod and vertebrate remains' (Cressler *et al.* 2010, p. 117) are

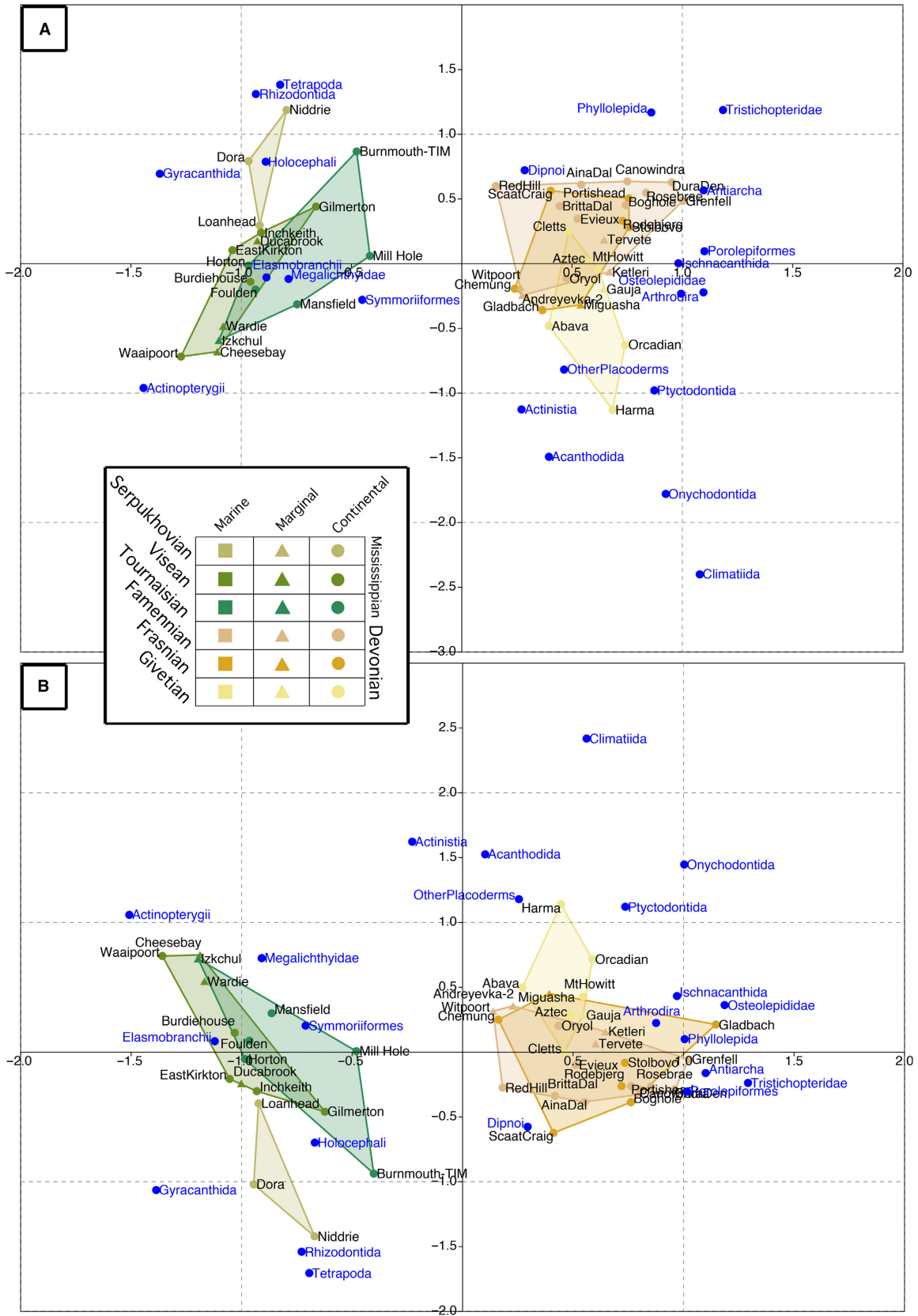


FIG. 16. Correspondence analysis results, non-marine sites only. A, raw diversity. B, relative diversity.

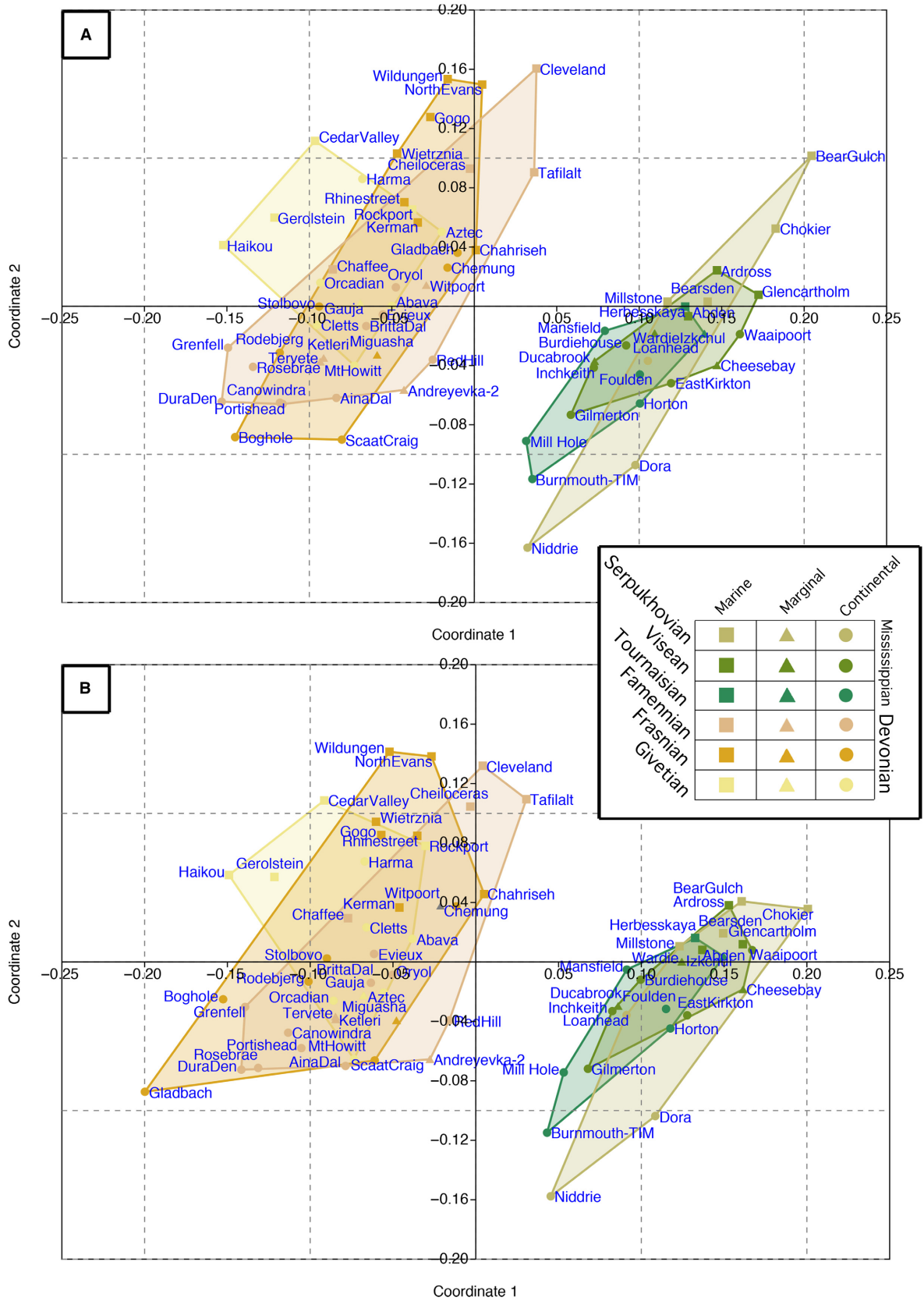


FIG. 17. Non-parametric multidimensional scaling results, full dataset. A, raw diversity. B, relative diversity.

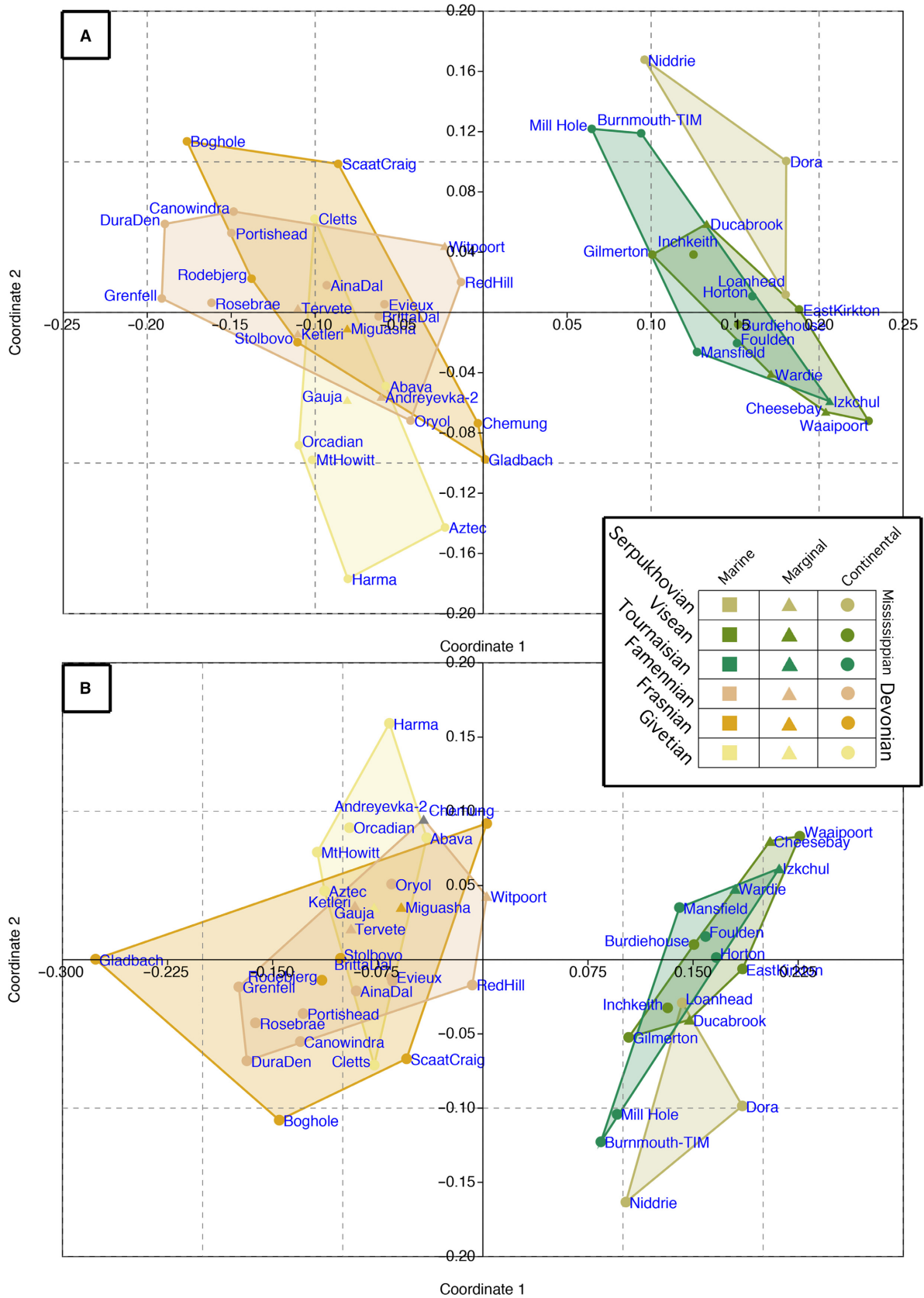


FIG. 18. Non-parametric multidimensional scaling results, non-marine sites only. A, raw diversity. B, relative diversity.

analogous to sandy siltstones. This emphasizes the ecological and preservational importance of these environments in the Devonian–Carboniferous.

Between flood episodes, laminated grey siltstones were deposited from suspension within shallow floodplain lakes. After the last sandy siltstone bed, lacustrine conditions were re-established with clastic input of siltstones and thin sand beds, perhaps derived from small sheet-floods into the lake. Inceptisols and large desiccation cracks formed by sub-aerial exposure of the lake and scrubby vegetation growth on the floodplain. Finally, the vertisol represents the formation of a more established soil, due either to the growth of vegetation under relatively dry, long-lived conditions or to a drop in the local water table/infilling of the water body by sediment. Roots recorded from vertisols in the Ballagan Formation can be up to 1 m in depth and are interpreted as having been formed by isolated stands of lycopsid trees (Kearsey *et al.* 2016).

Micropalaeontology interpretation

The variation within the microfossil assemblages illustrates the different palaeoenvironmental and taphonomic histories of each of the beds. Taking into account the breakage of some ostracod specimens during pedogenesis, the ostracod assemblage within the palaeosol is indicative of an autochthonous deposit due to the presence of juveniles, adults and carapaces (Boomer *et al.* 2003). The ostracods represent one of the oldest brackish-water floodplain assemblages of this group (Williams *et al.* 2005, 2006), although solely freshwater genera such as *Carbonita* that occur in the Visean (Bennett *et al.* 2012) are absent. A brackish salinity for this bed is consistent with the formation of the gleyed inceptisol under water-logged brackish conditions (Kearsey *et al.* 2016). The habitat of the ostracods may have been a saline marsh or pool on the floodplain.

The dominance of rhizodont microfossils within the *Aytonerpeton* bed is unusual for Ballagan Formation sandy siltstone beds, in which actinopterygian (macro)fossils are more common than rhizodonts (Bennett *et al.* 2016). This is the most rhizodont-rich bed observed within the Burnmouth succession to date. The evidence of clasts and flow-aligned plant debris within the bed indicates the transport of all fossil material, although the articulated nature of some specimens (e.g. the *Aytonerpeton* holotype, rhizodont vertebral series, lungfish skeleton) indicates local transportation distances. The original habitat of the fauna within this bed was likely to have been floodplain pools, lakes or land surfaces, where animals may have died in periods of drought. The abundance of plant material within the sandy siltstone beds indicates vegetated

floodplains, and rooting structures indicate scrubby vegetation to forested landscapes (Kearsey *et al.* 2016). Heavy rainfall on the floodplain then transported the fossil and plant material in a mud-supported debris flow, to be deposited within a floodplain lake. The microfossil sample 3 assemblage represents quieter deposition within a floodplain lake, affected by desiccation, then subject to one small flood event that infilled the desiccation cracks.

In the Carboniferous, many groups of actinopterygians, as well as rhizodonts, have been found in palaeoenvironments that span salinity gradients, suggesting that they were euryhaline or brackish–freshwater tolerant at this time (Carpenter *et al.* 2014, 2015; Ó Gogáin *et al.* 2016). Early Carboniferous eurypterids are mostly restricted to brackish or freshwater environments (Braddy 2001; Lamsdell & Braddy 2010). A brackish habit was recently confirmed for the Famennian East Greenland tetrapods, long considered to have been part of a freshwater fauna (Goedert *et al.* 2018). The microfossil content of the three samples is different from that identified from two dolostone beds from the Ballagan Formation on the Isle of Bute, which contain actinopterygians, sarcopterygians, dipnoans, elasmobranchs and non-gyracanth acanthodians (Carpenter *et al.* 2014). The latter two groups are absent from the TIM, as are *Chondrites* and *Phycosiphon*-like burrows, which are common within the dolostones (Bennett *et al.* 2017). The dolostones are thought to form in saline, coastal lakes subject to periodic influx of marine waters in storms. Burrows are not commonly identified within sandy siltstones in this formation (Bennett *et al.* 2016), however some fossils do indicate a marine influence. Palaeozoic *Spirorbis* has been interpreted to be of a marine origin, with a mechanism of larval transport onto coastal floodplains attributed to transport during storms or by tides (Gierlowski-Kordesch & Cassle 2015). It is likely that the laminated grey siltstone deposit was formed in a floodplain lake that was influenced by a relatively minor marine input.

Palaeoecology

The TIM fauna lived on a vegetated floodplain, centred in and around water bodies. The vertebrates were actinopterygians, holocephalan and gyracanth chondrichthyans, and several kinds of sarcopterygians: rhizodonts, lungfish and tetrapods (Table 1; Fig. 19). Living alongside them were eurypterids and myriapods (Smithson *et al.* 2012), as well as various microinvertebrates. Rhizodonts would have been the apex predators, presumably feeding on other taxa as well as each other. It is likely that gyracanth fed on small prey in the water column, whereas tetrapods were probably demersal faunivores, and possibly semiaquatic as well. Lungfish and

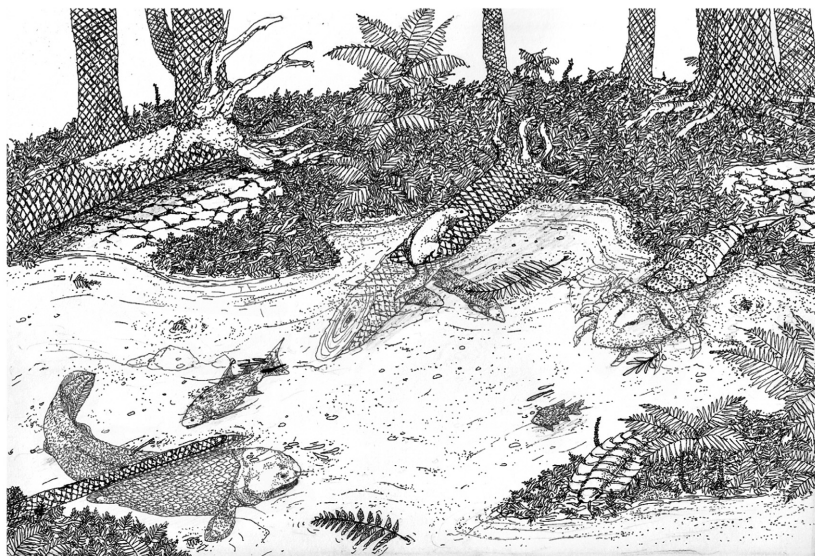


FIG. 19. Reconstruction of the Burnmouth TIM fauna. From left to right: rhizodont, gyracanth, tetrapod, actinopterygian, myriapod (lower), and eurypterid (upper). Artwork by Yasmin Yonan (University of Leicester, 2015).

holocephalans would have taken a range of prey, probably overlapping in their consumption with the sediment-mining eurypterids. Myriapods lived on land, consuming plants and available organic detritus.

The ecological relationships that are emerging from within the Ballagan Formation (CEB unpub. data) emphasize the role of diversifying non-marine invertebrates in providing a wider base for Carboniferous biotas relative to Devonian ones. Several lines of evidence are consistent with this hypothesis. The taxonomic diversification of holocephalans (Sallan *et al.* 2011; Richards *et al.* 2018) and lungfish (Smithson *et al.* 2015) during the Tournaisian and Visean has been noted previously. In this context it is worth noting that toothplates are highly effective in immobilizing elusive, soft-bodied prey through massive trauma (MIC pers. obs.) and that on examination, multiple Early Carboniferous holocephalans have previously neglected marginal dentition. These suggest that multiple taxa took advantage of an increasing abundance and diversity of small invertebrate prey. This hypothesis should be explored further as more fossils are described from the Ballagan and other Tournaisian deposits.

The consistency in taxonomic identities and numerical proportions in the micro- and macrofossil samples (Otoo *et al.* 2018, micropalaeontology data) suggests that there is a common signal being captured by both. In particular, the low number of actinopterygian specimens and large number of rhizodont specimens probably at least somewhat reflect genuine paucity and abundance rather than solely preservation bias. Both a single actinopterygian and a single rhizodont will produce numerous scales with high preservation potential, and that the TIM rhizodonts are so much more in evidence than the actinopterygians is striking. However, low relative abundance and diversity

of actinopterygians is a common feature of both Devonian and Carboniferous non-marine settings (Cressler *et al.* 2010; Sallan & Coates 2010; Carpenter *et al.* 2015; Ó Gogáin *et al.* 2016); at least through the early part of the Late Carboniferous, the increasing taxonomic, morphological and ecological diversity of actinopterygians is considered to be largely a brackish and, in particular, marine phenomenon (Sallan & Coates 2010, 2013). More abundant and morphologically diverse actinopterygians have been reported from Blue Beach, where the succession preserves multiple marine incursions (Mansky & Lucas 2013).

The rhizodont occurrences in the TIM fit a broader pattern. Rhizodonts are often represented by two species in Carboniferous localities (Sallan & Coates 2010; Carpenter *et al.* 2014, 2015; Ó Gogáin *et al.* 2016). Common associations are *Archichthys/Strepsodus* and *Screbinodus/Rhizodus*, which has long had a confounding effect on the taxonomy of these genera (Andrews 1985; Jeffery 2006). *Screbinodus* is a small rhizodont, with a length of 1.5–2 m; *Strepsodus* and *Rhizodus* are both large rhizodonts, with length estimates of 3–5 and 5–7 m, respectively (Jeffery 2012). Given the limited material, size estimates have not been produced for *Archichthys*. The TIM *Strepsodus* material indicates individuals across a range of sizes, the largest probably about 1 m in length. This parallels the rhizodonts of the Foulden locality, where Andrews (1985) identified multiple ‘small form’ individuals that she suggested were juveniles of the ‘large form’ that lived elsewhere; all these were later referred to *Strepsodus* by Jeffery (2006). This suggests that size was an important ecological discriminant both within and between rhizodont species.

The small size of the referred lungfish toothplates might appear to support Sallan & Galimberti’s (2015)

conclusion of a post-Devonian size reduction. However, 35 m above the Devonian/Carboniferous boundary at Burnmouth there is evidence of both very small and very large lungfish, with very large lungfish also occurring 20 m above the TIM (TRS pers. obs.; T. Challands unpub. data; Clack *et al.* 2018). There are also gyracanth and rhizodont fossils from outside the TIM that represent larger individuals (BKAO pers. obs.) Therefore, it does not seem likely that organisms experienced concerted size reduction at the extinction or in its aftermath. Further sampling will allow greater examination of this hypothesis.

Faunal analyses

The diversity and taxonomic composition of the Mill Hole fauna is most similar to that of the TIM (Carpenter *et al.* 2014), including at least one shared species of rhizodont (*Strepsodus sauroides*). Mill Hole is also in the Ballagan Formation and roughly coeval with the TIM, and these qualitative observations indicate that these assemblages sample a coherent 'Ballagan fauna' (this study; CEB unpub. data) However, unlike the TIM, the Mill Hole fauna is derived from a dolostone as opposed to a siltstone. The fauna also contains the elasmobranch *Ageleodus* and the sarcopterygian *Megalichthys* (Carpenter *et al.* 2014); while the actinopterygian material is similar in terms of content (mostly scales and lepidotrichia) it is the most abundant material at the locality (JAC pers. obs.) These details indicate that Mill Hole is taxonomically and geologically sampling a more marine signal than the TIM.

The persistent recovery of a Devonian/Carboniferous split when the entire dataset is analysed with both CA and NMDS supports the conclusion of Sallan & Coates (2010). The persistence of this split when the marine sites are removed suggests that the end-Devonian extinction has a diversity signal in both marine and non-marine settings. However, the losses were not evenly distributed among groups; placoderms account for four of the taxonomic divisions within this dataset and were eliminated completely at the end of the Devonian. The Carboniferous non-marine gyracanth–rhizodont–tetrapod association recovered by the correspondence analysis was already in place in the Late Devonian, there often accompanied by tristichopterids and lungfish (Cressler *et al.* 2010), and usually porolepiformes and antiarchs as well. In non-marine settings the end-Devonian extinction left behind a faunal subset which does not seem to have been greatly disturbed. On either side of the Devonian–Carboniferous boundary, rhizodonts are generally represented by the same number of species per locality and tetrapods greatly increase in diversity relative to the Devonian. The fact that, when marine sites are removed, holocephalans

are associated with gyracanth, rhizodonts and tetrapods (as is the case in the TIM) as opposed to the more marine-inclined actinopterygians, elasmobranchs and symmoriiformes, is interesting and may suggest different environmental trajectories for elasmobranchs and holocephalans in the Early Carboniferous.

The TIM and Devonian–Carboniferous faunal assembly

The TIM (vertebrate) fauna is very similar to that of the Famennian Red Hill locality, as are their respective environments: both are coastal alluvial plains at low palaeolatitude, though Burnmouth experienced greater rainfall (Retallack *et al.* 2009; Kearsy *et al.* 2016). Indeed, the only major vertebrate division not represented in similar numbers in the TIM as at Red Hill are elasmobranchs (ctenacanth) and placoderms (Cressler *et al.* 2010). Conversely, holocephalans are absent from Red Hill. The rest of the fauna in both cases is composed of gyracanth, tetrapods, actinopterygians, lungfish and large predatory sarcopterygians (including rhizodonts). The Famennian vertebrate fauna from East Greenland, famous for *Acanthostega* and *Ichthyostega*, also has a similar composition (Blom *et al.* 2007). It appears that the TIM is sampling a faunal–environmental association that apparently passed through the end-Devonian extinction without extensive modification.

Much of this fauna is held in common with 'typical' Carboniferous coal swamp faunas such as Dora and Niddrie, and floodplain localities such as Gilmerton (Sallan & Coates 2010), their qualitative affinities supported by the results of the faunal analyses. The only characteristic coal swamp taxon missing from the TIM are xenacanth, which first appear in the Visean with *Diplodoselache* at Wardie (this may be superseded by Tournaisian occurrences at Burnmouth; Clack *et al.* 2018) It would be interesting to know the extent to which the apparent transition of the more or less Devonian-type floodplain fauna (as seen at Red Hill, East Greenland and, with minor changes, in the TIM at Burnmouth) to the coal swamp setting represents a physical move inland toward fresher water or if the swamps developed on top of the existing alluvial plains (the two scenarios are not mutually exclusive). With the addition of xenacanth, the key difference between the floodplain faunal association and the coal swamp association seems to be the increased abundance and diversity of tetrapods (and arthropods), at least in part driven by the increased resources and complexity of terrestrial habitats. But overall, much of the non-marine faunal order in the Carboniferous can be described as expansion of a discernable, pre-existing subset of Devonian diversity. This contrasts with marine environments, where, following the extinction of placoderms, the fauna diversified greatly with the addition of large clades/

taxonomic divisions (Coates *et al.* 2017, 2018; Giles *et al.* 2017) to create very differently-composed marine faunas compared to those that existed in the Devonian.

Yao *et al.* (2015) recovered isotope excursions in carbon and nitrogen from which they infer sea level fluctuations with a net drop through the Tournaisian, particularly in the second half of the stage. These changes begin in the mid-Tournaisian and do not stabilize until the early Viséan. Further investigation of Tournaisian environments preserved at Burnmouth and elsewhere is needed to determine the environmental and biological impact of these sea level changes. The presence of macrofossil assemblages throughout the Ballagan at Burnmouth, starting from very near the Devonian–Carboniferous boundary, indicates that floodplain biotas were able to persist through these continued post-extinction environmental changes. The physical and physiological ability to move between different salinity regimes would doubtless have been useful, and this interval may be responsible for encouraging the apparent retention of euryhalinity in many vertebrates throughout the Carboniferous.

It is not obvious to what extent these faunal transitions were accompanied by ecological restructuring. Placoderms were extremely numerous at Red Hill, East Greenland and other Late Devonian localities, and had a diversity of morphologies and feeding ecologies; their extinction at the end of the Devonian must have had ecological impacts, but what those were is currently unclear. Also unknown are the impacts of the increased diversity and terrestrialization of tetrapods and arthropods during the Carboniferous. Future comparative ecological work will be valuable for understanding these issues.

CONCLUSIONS

Despite post-dating the end-Devonian mass extinction by only a few million years, the TIM fauna contains multiple invertebrate and vertebrate taxa across different ecological roles. As in environmentally similar Late Devonian assemblages, actinopterygians are low in diversity and abundance, with the assemblage dominated numerically and taxonomically by sarcopterygians. The TIM lacks the placoderms of the Devonian and the tetrapod diversity and xenacanth found in later Carboniferous biotas, but otherwise seems to represent a floodplain faunal association that persisted from the Late Devonian into the Carboniferous. Either ecologically or evolutionarily, this floodplain association may have formed the basis of the coal swamp faunas that characterize many Carboniferous localities. Insofar as the Carboniferous is marked by a diversification of actinopterygians and elasmobranchs, during the Tournaisian these events may have been happening in different environmental or faunal contexts (Mansky & Lucas 2013).

This study and other work (Mansky & Lucas 2013; Carpenter *et al.* 2014; Anderson *et al.* 2015; Clack *et al.* 2016) have focused primarily on taxonomic and phylogenetic changes through the Devonian–Carboniferous transition and Romer’s Gap. These data are providing a basis for future work linking taxonomy and phylogeny to ecology, which will provide an enhanced perspective on the biological and environmental changes through this important period in Earth history.

Acknowledgements. This work was funded by NERC consortium grants NEJ021067/1 (BGS), NE/J022713/1 (Cambridge), NE/J020729/1 (Leicester), NE/J020621/1 (NMS), and NE/J021091/1 (Southampton), as well as an Evan Carroll Commager Fellowship for Graduate Study in Paleontology from Amherst College. Most of this research was conducted by BKAO in 2014–2015 for an MPhil project under the supervision of JAC at the University of Cambridge. We thank Anne Brown and Colin MacFadyen at Scottish Natural Heritage for permission to collect at Site of Special Scientific Interest under their care, Paul Banks from the Edinburgh office of The Crown Estate for permission to collect from the foreshore at Burnmouth, members of the TW:eed Project team for help and support during the excavation of the Burnmouth site, Sarah Finney and the Department of Earth Sciences, University of Cambridge, for help and guidance and the use of lab facilities during the preparation of the bulk samples recovered from Burnmouth, Keturah Smithson for scanning the specimens and help with preparing the rendered images, Nick Fraser and Stig Walsh (NMS) and Matt Lowe (UMZC) for collections access, and the community of Burnmouth for their support and interest during the TW:eed Project. Yasmin Yonan (University of Leicester) provided the reconstruction of the Burnmouth fauna. Graham Slater provided valuable advice on computational methods. TIK publishes with the permission of the Executive Director, British Geological Survey (NERC). Two anonymous referees commented on an earlier version of the manuscript.

DATA ARCHIVING STATEMENT

Data for this study, including faunal diversity datasets and micropalaeontological data, are available in the Dryad Digital Repository: <https://doi.org/10.5061/dryad.j5t58j4>

Editor. Marcello Ruta

REFERENCES

- ANDERSON, J. S., SMITHSON, T. R., MANSKY, C. F., MEYER, T. and CLACK, J. A. 2015. A diverse tetrapod fauna at the base of ‘Romer’s Gap’. *PLoS One*, **10**, 1–27.
- ANDREWS, S. M. 1985. Rhizodont crossopterygian fish from the Dinantian of Foulden, Berwickshire, Scotland, with a re-evaluation of this group. *Transactions of the Royal Society of Edinburgh: Earth Sciences*, **76**, 67–95.

- and WESTOLL, T. S. 1970. XII.—The postcranial skeleton of Rhipidistian fishes excluding Eusthenopteron. *Transactions of the Royal Society of Edinburgh: Earth Sciences*, **68**, 391–489.
- BENNETT, C. E., SIVETER, D. J., DAVIES, S. J., WILLIAMS, M., WILKINSON, I. P., BROWNE, M. A. E. and MILLER, C. G. 2012. Ostracods from freshwater and brackish environments of the Carboniferous of the Midland Valley of Scotland: the early colonization of terrestrial water bodies. *Geological Magazine*, **149**, 366–396.
- KEARSEY, T. I., DAVIES, S. J., MILLWARD, D., CLACK, J. A., SMITHSON, T. R. and MARSHALL, J. E. A. 2016. Early Mississippian sandy siltstones preserve rare vertebrate fossils in seasonal flooding episodes. *Sedimentology*, **63**, 1677–1700.
- HOWARD, A. S., DAVIES, S. J., KEARSEY, T. I., MILLWARD, D., BRAND, P. J., BROWNE, M. A. E., REEVES, E. J. and MARSHALL, J. E. A. 2017. Ichnofauna record cryptic marine incursions onto a coastal floodplain at a key Lower Mississippian tetrapod site. *Palaeogeography, Palaeoclimatology, Palaeoecology*, **468**, 287–300.
- BINNEY, E. W. 1841. On the fossil fishes of the Pendleton coal field. *Transactions of the Manchester Geological Society*, **1**, 153–178.
- BLOM, H., CLACK, J. A., AHLBERG, P. E. and FRIEDMAN, M. 2007. Devonian vertebrates from East Greenland: a review of faunal composition and distribution. *Geodiversitas*, **29**, 119–141.
- BONAPARTE, C. L. 1831. Saggio di una distribuzione metodica degli animali vertebrati. *Giornale Arcadico di Scienze*, **49**, 1–77.
- BOOMER, I., HORNE, D. J. and SLIPPER, I. J. 2003. The use of ostracods in palaeoenvironmental studies, or what can you do with an ostracod shell? 153–179. In PARK, L. E. and SMITH, A. J. (eds). *Bridging the gap: Trends in the ostracode biological and geological sciences*. The Paleontological Society Papers, **9**.
- BRADDY, S. J. 2001. Eurypterid palaeoecology: palaeobiological, ichnological and comparative evidence for a ‘mass-moultmate’ hypothesis. *Palaeogeography, Palaeoclimatology, Palaeoecology*, **172**, 115–132.
- BRAY, J. R. and CURTIS, J. T. 1957. An ordination of the Upland Forest communities of Southern Wisconsin. *Ecological Monographs*, **27**, 325–349.
- BRAZEAU, M. D. 2005. A new genus of rhizodontid (Sarcopterygii, Tetrapodomorpha) from the Lower Carboniferous Horton Bluff Formation of Nova Scotia, and the evolution of the lower jaws in this group. *Canadian Journal of Earth Sciences*, **42**, 1481–1499.
- CARPENTER, D., FALCON-LANG, H. J., BENTON, M. J. and NELSON, W. J. 2011. Fishes and tetrapods in the Upper Pennsylvanian (Kasimovian) Cohn Coal Member of the Mattoon Formation of Illinois, United States: systematics, paleoecology, and paleoenvironments. *Palaio*, **26**, 639–657.
- CARPENTER, D. K., FALCON-LANG, H. J., BENTON, M. J. and HENDERSON, E. 2014. Carboniferous (Tournaisian) fish assemblages from the Isle of Bute, Scotland: systematics and palaeoecology. *Palaeontology*, **57**, 1215–1240.
- — — and GREY M. 2015. Early Pennsylvanian (Langsettian) fish assemblages from the Joggins Formation, Canada, and their implications for palaeoecology and palaeogeography. *Palaeontology*, **58**, 661–690.
- CLACK, J. A. 2002. An early tetrapod from ‘Romer’s Gap’. *Nature*, **418**, 72–76.
- and FINNEY, S. M. 2005. *Pederpes finneyae*, an articulated tetrapod from the Tournaisian of Western Scotland. *Journal of Systematic Palaeontology*, **2**, 311–346.
- BENNETT, C. E., CARPENTER, D. K., DAVIES, S. J., FRASER, N. C., KEARSEY, T. I., MARSHALL, J. E. A., MILLWARD, D., OTOO, B. K. A., REEVES, E. J., ROSS, A. J., RUTA, M., SMITHSON, K. Z., SMITHSON, T. R. and WALSH, S. A. 2016. Phylogenetic and environmental context of a Tournaisian tetrapod fauna. *Nature Ecology & Evolution*, **1**, 1–11.
- — DAVIES, S. J., SCOTT, A. C., SHERWIN, J. and SMITHSON, T. R. 2018. A Tournaisian (earliest Carboniferous) conglomerate-preserved non-marine faunal assemblage and its environmental and sedimentological context. *PeerJ Preprints*, **6**, e27102v1. <https://doi.org/10.7287/peerj.preprints.27102v1>
- CLARKSON, E. N. K. 1985. Palaeoecology of the Dinantian of Foulden, Berwickshire, Scotland. *Transactions of the Royal Society of Edinburgh: Earth Sciences*, **76**, 97–100.
- MILNER, A. R. and COATES, M. I. 1994. Palaeoecology of the Viséan of East Kirkton, West Lothian, Scotland. *Transactions of the Royal Society of Edinburgh: Earth Sciences*, **84**, 417–425.
- COATES, M. I. and CLACK, J. A. 1995. Romer’s Gap: tetrapod origins and terrestriality. *Bulletin du Muséum national d’Histoire naturelle C*, **17**, 373–388.
- GESS, R. W., FINARELLI, J. A., CRISWELL, K. E. and TIETJEN, K. 2017. A symmoriiform chondrichthyan braincase and the origin of chimaeroid fishes. *Nature*, **541**, 208–211.
- FINARELLI, J. A., SANSOM, I. J., ANDREEV, P. S., CRISWELL, K. E., TIETJEN, K., RIVERS, M. L. and LA RIVIERE, P. J. 2018. An early chondrichthyan and the evolutionary assembly of a shark body plan. *Proceedings of the Royal Society B*, **285**, 20172418.
- COPE, E. D. 1887. *The origin of the fittest*. Appleton, New York, 536 pp.
- CRESSLER, W. L., DAESCHLER, E. B., SLINGERLAND, R. and PETERSON, D. A. 2010. Terrestrialization in the Late Devonian: a palaeoecological overview of the Red Hill site, Pennsylvania, USA. *Geological Society, London, Special Publications*, **339**, 111–128.
- DAESCHLER, E. B. 2000. An early actinopterygian fish from the Catskill formation (Late Devonian, Famennian) in Pennsylvania, USA. *Proceedings of the Academy of Natural Sciences of Philadelphia*, **150**, 181–192.
- DAVIS, M. C., SHUBIN, N. H. and DAESCHLER, E. B. 2001. Immature rhizodontids from the Devonian of North America. *Bulletin of the Museum of Comparative Zoology*, **156**, 173–187.
- FALCON-LANG, H. J. 1999. The Early Carboniferous (Courseyan–Arundian) monsoonal climate of the British Isles:

- evidence from growth rings in fossil woods. *Geological Magazine*, **136**, 177–187.
- FRIEDMAN, M. and BLOM, H. 2006. A new actinopterygian from the Famennian of East Greenland and the interrelationships of Devonian ray-finned fishes. *Journal of Paleontology*, **80**, 1186–1204.
- and SALLAN, L. C. 2012. Five hundred million years of extinction and recovery: a Phanerozoic survey of large-scale diversity patterns in fishes. *Palaentology*, **55**, 707–742.
- GARVEY, J. M., JOHANSON, Z. and WARREN, A. 2005. Redescription of the pectoral fin and vertebral column of the rhizodontid fish *Barameda decipiens* from the Lower Carboniferous of Australia. *Journal of Vertebrate Paleontology*, **25**, 8–18.
- GIERLOWSKI-KORDESCH, E. H. and CASSLE, C. F. 2015. The ‘*Spirorbis*’ problem revisited: sedimentology and biology of microconchids in marine-nonmarine transitions. *Earth-Science Reviews*, **148**, 209–227.
- GILES, S., XU, G. H., NEAR, T. J. and FRIEDMAN, M. 2017. Early members of ‘living fossil’ lineage imply later origin of modern ray-finned fishes. *Nature*, **549**, 265–268.
- GOEDERT, J., LÉCUYER, C., AMIOT, R., ARNAUD-GODET, F., WANG, X., CUI, L., CUNY, G., DOUAY, G., FOUREL, F., PANCZER, G., SIMON, L., STEYER, J. and ZHU, M. 2018. Euryhaline ecology of early tetrapods revealed by stable isotopes. *Nature*, **558**, 68–72.
- GOODRICH, E. S. 1930. *Studies on the structure and development of vertebrates*. Macmillan, London, 873 pp.
- GREIG, D. C. 1988. *Geology of the Eyemouth district*. Memoir of the British Geological Survey, Sheet 34.
- HAMMER, Ø. 2015. Palaeontological community and diversity analysis – brief notes. Paläontologisches Institut und Museum, Zürich, 1–36.
- HUXLEY, T. H. 1880. On the application of the laws of evolution to the arrangement of the Vertebrata and more particular the Mammalia. *Proceedings of the Zoological Society of London*, **1880**, 649–662.
- JEFFERY, J. E. 2006. The Carboniferous fish genera *Strepsodus* and *Archichthys* (Sarcopterygii: Rhizodontida): clarifying 150 years of confusion. *Palaentology*, **49**, 112–132.
- 2012. Cranial morphology of the Carboniferous rhizodontid *Screbinodus ornatus* (Osteichthyes: Sarcopterygii). *Journal of Systematic Palaeontology*, **10**, 475–519.
- JOHANSON, Z. and AHLBERG, P. E. 2001. Devonian rhizodontids and tristichopterids (Sarcopterygii; Tetrapodomorpha) from East Gondwana. *Earth & Environmental Science Transactions of the Royal Society of Edinburgh*, **92**, 43–74.
- KEARSEY, T. I., BENNETT, C. E., MILLWARD, D., DAVIES, S. J., GOWING, C. J. B., KEMP, S. J., LENG, M. J., MARSHALL, J. E. A. and BROWNE, M. A. E. 2016. The terrestrial landscapes of tetrapod evolution in earliest Carboniferous seasonal wetlands of SE Scotland. *Palaogeography, Palaeoclimatology, Palaeoecology*, **457**, 52–69.
- LAMSDALL, J. C. and BRADY, S. J. 2010. Cope’s Rule and Romer’s theory: patterns of diversity and gigantism in eurypterids and Palaeozoic vertebrates. *Biology Letters*, **6**, 265–269.
- LOMBARD, R. E. and BOLT, J. R. 1995. A new primitive tetrapod, *Whatcheeria deltae*, from the Lower Carboniferous of Iowa. *Palaentology*, **38**, 471–494.
- LONG, J. A. 1989. A new rhizodontiform fish from the Early Carboniferous of Victoria, Australia, with remarks on the phylogenetic position of the group. *Journal of Vertebrate Paleontology*, **9**, 1–17.
- MANSKY, C. F. and LUCAS, S. G. 2013. Romer’s Gap revisited: continental assemblages and ichno-assemblages from the basal Carboniferous of Blue Beach, Nova Scotia, Canada. *New Mexico Museum of Natural History & Science Bulletin*, **60**, 244–273.
- MICKLE, K. E. 2011. The Early Actinopterygian fauna of the Manning Canyon Shale Formation (Upper Mississippian, Lower Pennsylvanian) of Utah, U.S.A. *Journal of Vertebrate Paleontology*, **31**, 962–980.
- 2017. The lower actinopterygian fauna from the Lower Carboniferous Albert shale formation of New Brunswick, Canada – a review of previously described taxa and a description of a new genus and species. *Fossil Record*, **20**, 47–67.
- MÜLLER, J. 1845. Über den Bau und die Grenzen der Ganoiden, und über das natürliche System der Fische. *Abhandlungen der Königlichen Akademie der Wissenschaften zu Berlin*, **1844**, 117–216.
- Ó GOGÁIN, A., FALCON-LANG, H. J., CARPENTER, D. K., MILLER, R. F., BENTON, M. J., PUFUHL, P. K., RUTA, M., DAVIES, T. G., HINDS, S. J. and STIMSON, M. R. 2016. Fish and tetrapod communities across a marine to brackish salinity gradient in the Pennsylvanian (early Moscovian) Minto Formation of New Brunswick, Canada, and their palaeoecological and palaeogeographical implications. *Palaentology*, **59**, 689–724.
- OBRUCHEV, D. V. 1953. Studies on eestids and the works of A. P. Karpinski. *U.S.S.R. Academy of Sciences, Works of the Palaeontological Institute*, **45**, 1–86.
- OTOO, B. K. A., CLACK, J. A., SMITHSON, T. R., BENNETT, C. E., KEARSEY, T. I. and COATES, M. I. 2018. Data from: A fish and tetrapod fauna from Romer’s Gap preserved in Scottish Tournaisian floodplain deposits. *Dryad Digital Repository*. <https://doi.org/10.5061/dryad.j5t58j4>
- PARDO, J. D., SZOSTAKIWSKYJ, M., AHLBERG, P. E. and ANDERSON, J. S. 2017. Hidden morphological diversity among early tetrapods. *Nature*, **546**, 642–645.
- PATTERSON, C. 1965. The phylogeny of the chimaeroids. *Philosophical Transactions of the Royal Society B*, **249**, 109–219.
- RESTALLACK, G. J., HUNT, R. R. and WHITE, T. S. 2009. Late Devonian tetrapod habitats indicated by palaeosols in Pennsylvania. *Journal of the Geological Society*, **166**, 1143–1156.
- RICHARDS, K., SHERWIN, J., SMITHSON, T. R., BENNION, R., DAVIES, S. J., MARSHALL, J. and CLACK, J. A. 2018. Diverse and durophagous: early Carboniferous chondrichthyans from the Scottish Borders. *Earth & Environmental Science Transactions of the Royal Society of Edinburgh*, **108**, 67–87.
- ROMER, A. S. 1955. Herpetichthyes, Amphibioidi, Chonichthyes or Sarcopterygii? *Nature*, **176**, 126.

- 1956. The early evolution of land vertebrates. *Proceedings of the American Philosophical Society*, **100**, 157–167.
- RUST, B. R. and NANSON, G. C. 1989. Bedload transport of mud as pedogenic aggregates in modern and ancient rivers. *Sedimentology*, **36**, 291–306.
- SALLAN, L. C. 2014. Major issues in the origins of ray-finned fish (Actinopterygii) biodiversity. *Biological Reviews*, **89**, 950–971.
- and COATES, M. I. 2010. End-Devonian extinction and a bottleneck in the early evolution of modern jawed vertebrates. *Science*, **107**, 10131–10135.
- — 2013. Styracopterid (Actinopterygii) ontogeny and the multiple origins of post-Hangenberg deep-bodied fishes. *Zoological Journal of the Linnean Society*, **169**, 156–199.
- SALLAN, L. and GALIMBERTI, A. K. 2015. Body-size reduction in vertebrates following the end-Devonian mass extinction. *Science*, **350**, 812–815.
- SALLAN, L. C., KAMMER, T. W., AUSICH, W. I. and COOK, L. A. 2011. Persistent predator–prey dynamics revealed by mass extinction. *Proceedings of the National Academy of Sciences*, **108**, 8335–8338.
- SCHINDLER, T. 2018. Revision of *Rhabdolepis macropterus* (Bronn, 1829) (Osteichthyes, lower Actinopterygii; Lower Permian, SW Germany). *PalZ*, 10 pp. <https://doi.org/10.1007/s12542-018-0410-z>
- SMITH, M. M., SMITHSON, T. R. and CAMPBELL, K. S. W. 1987. The relationships of *Uronemus*: a carboniferous dipnoan with highly modified tooth plates. *Philosophical Transactions of the Royal Society B*, **317**, 299–327.
- SMITHSON, T. R. 1982. The cranial morphology of *Greererpeton burkemorani* Romer (Amphibia: Temnospondyli). *Journal of the Linnean Society of London, Zoology*, **76**, 29–90.
- WOOD, S. P., MARSHALL, J. E. A. and CLACK, J. A. 2012. Earliest Carboniferous tetrapod and arthropod faunas from Scotland populate Romer's Gap. *Proceedings of the National Academy of Sciences*, **109**, 4532–4537.
- RICHARDS, K. R. and CLACK, J. A. 2015. Lungfish diversity in Romer's Gap: reaction to the end-Devonian extinction. *Palaeontology*, **59**, 29–44.
- SNYDER, D. 2011. Gyracanthid gnathostome remains from the Carboniferous of Illinois. *Journal of Vertebrate Paleontology*, **31**, 902–906.
- STAHL, B. J. 1999. Chondrichthyes III: Holocephali. 1–164. In SCHULTZE, H.-P. (ed.) *Handbook of Paleichthyology*. Vol. 4. Friedrich Pfeil, Munich, 164 pp.
- SWEETMAN, S. C. and INSOLE, A. N. 2010. The plant debris beds of the Early Cretaceous (Barremian) Wessex Formation of the Isle of Wight, southern England: their genesis and palaeontological significance. *Palaeogeography, Palaeoclimatology, Palaeoecology*, **292**, 409–424.
- TRAQUAIR, R. H. 1873. On *Phaneropleuron andersoni* Huxley and *Uronemus lobatus* Agassiz. *Journal of the Royal Geological Society of Ireland*, **3**, 41–47.
- TURNER, S., BURROW, C. J. and WARREN, A. 2005. *Gyracanthides hawkinsi* sp. nov. (Acanthodii, Gyracanthidae) from the Lower Carboniferous of Queensland, Australia, with a review of gyracanthid taxa. *Palaeontology*, **48**, 963–1006.
- WAKELIN-KING, G. A. and WEBB, J. A. 2007a. Upper-flow-regime mud floodplains, lower-flow-regime sand channels: sediment transport and deposition in a drylands mud-aggregate river. *Journal of Sedimentary Research*, **77**, 702–712.
- — 2007b. Threshold-dominated fluvial styles in an arid-zone mud-aggregate river: the uplands of Fowlers Creek, Australia. *Geomorphology*, **85**, 114–127.
- WARREN, A., CURRIE, B. P., BURROW, C. J. and TURNER, S. 2000. A redescription and reinterpretation of *Gyracanthides murrayi* Woodward 1906 (Acanthodii, Gyracanthidae) from the Lower Carboniferous of the Mansfield Basin, Victoria, Australia. *Journal of Vertebrate Paleontology*, **20**, 225–242.
- WELLSTEAD, C. F. 1982. A Lower Carboniferous aistopod amphibian from Scotland. *Palaeontology*, **25**, 193–208.
- WILLIAMS, M., STEPHENSON, M., WILKINSON, I. A. N. P., LENG, M. J. and MILLER, C. G. 2005. Early Carboniferous (Late Tournaisian–Early Viséan) ostracods from the Ballagan Formation, central Scotland, UK. *Journal of Micropalaeontology*, **24**, 77–94.
- LENG, M. J., STEPHENSON, M. H., ANDREWS, J. E., WILKINSON, I. P., SIVETER, D. J., HORNE, D. J. and VANNIER, J. M. C. 2006. Evidence that Early Carboniferous ostracods colonised coastal flood plain brackish water environments. *Palaeogeography, Palaeoclimatology, Palaeoecology*, **230**, 299–318.
- WILSON, C. D., PARDO, J. D. and ANDERSON, J. S. 2018. A primitive actinopterygian braincase from the Tournaisian of Nova Scotia. *Proceedings of the Royal Society B*, **5**, 171727.
- YAO, L., QIE, W., LUO, G., LIU, J., ALGEO, T. J., BAI, X., YANG, B. and WANG, X. 2015. The TICE event: perturbation of carbon–nitrogen cycles during the mid-Tournaisian (Early Carboniferous) greenhouse–icehouse transition. *Chemical Geology*, **401**, 1–14.
- ZHU, M., AHLBERG, P. E., ZHAO, W. J. and JIA, L. T. 2017. A Devonian tetrapod-like fish reveals substantial parallelism in stem tetrapod evolution. *Nature Ecology & Evolution*, **1**, 1470–1476.